

**TEMPERATURE REDUCTION IN BUILDINGS
BY GEOTHERMAL AIR COOLING SYSTEM**

LIM CHEE XUAN

UNIVERSITI TUNKU ABDUL RAHMAN

**TEMPERATURE REDUCTION IN BUILDINGS BY GEOTHERMAL AIR
COOLING SYSTEM**

LIM CHEE XUAN

**A project report submitted in partial fulfilment of the
requirements for the award of Bachelor of Engineering
(Hons.) Mechanical Engineering**

**Faculty of Engineering and Science
Universiti Tunku Abdul Rahman**

May 2015

DECLARATION

I hereby declare that this project report is based on my original work except for citations and quotations which have been duly acknowledged. I also declare that it has not been previously and concurrently submitted for any other degree or award at UTAR or other institutions.

Signature : _____

Name : LIM CHEE XUAN

ID No. : 10UEB03546

Date : _____

APPROVAL FOR SUBMISSION

I certify that this project report entitled “**TEMPERATURE REDUCTION IN BUILDINGS BY GEOTHERMAL AIR COOLING SYSTEM**” was prepared by **LIM CHEE XUAN** has met the required standard for submission in partial fulfilment of the requirements for the award of Bachelor of ENGINEERING (Hons.) MECHANICAL ENGINEERING at Universiti Tunku Abdul Rahman.

Approved by,

Signature : _____

Supervisor : DR. LIANG MENG SUAN

Date : _____

The copyright of this report belongs to the author under the terms of the copyright Act 1987 as qualified by Intellectual Property Policy of Universiti Tunku Abdul Rahman. Due acknowledgement shall always be made of the use of any material contained in, or derived from, this report.

© 2015, LIM CHEE XUAN. All right reserved.

Specially dedicated to
my beloved Parents, Siblings and God Almighty

ACKNOWLEDGEMENTS

I would like to thank everyone who had contributed to the successful completion of this project. I would like to express my gratitude to my research supervisor, Dr. Liang Meng Suan and research co-supervisor, Dr. Tan Yong Chai for their invaluable advice, guidance and their enormous patience throughout the development of the research.

In addition, I would also like to express my gratitude to my loving parents, siblings and friends who had helped and given me encouragement to complete this final year project.

Last but not least, I am also in debt to Faculty of Engineering and Science of University Tunku Abdul Rahman for the usage of Civil Laboratory, Mechatronics Laboratory and Mechanical Workshop for analytical study purpose. My sincere appreciation also extends to all my colleagues, housemates, and friends whom had provided assistance at various occasions.

Finally, to individuals who has involved neither directly nor indirectly in succession of this thesis. Indeed, I could never adequately express my indebtedness to all of them. Thank you.

TEMPERATURE REDUCTION IN BUILDINGS BY GEOTHERMAL AIR COOLING SYSTEM

ABSTRACT

This report describes in details the Temperature Reduction in Buildings by Geothermal Air Cooling System, concentrating on material selection for piping system, ground loop design of underground heat exchanger and coefficient of performance (COP) of the cooling system using the material selected. The aim of this report is to achieve temperature reduction in buildings by implementation of geothermal air cooling system in Malaysia using new piping materials. The detail and properties of the four materials are listed in Chapter 3. The method for choosing the best material for geothermal air cooling system are also being discussed in Chapter 3. The material for piping system is determined by comparing four type of materials available in the market in terms of thermal conductivity, cost and availability in the market in Malaysia. In a nutshell, 8.3 m of polyvinyl chloride (PVC) pipe with outer diameter of 80 mm has been chosen to be the material for the construction of piping system for its relatively cheap price and practically superior thermal conductivity.

The geothermal cooling system designed and installed shows a high coefficient of performance (COP) of 6.76, and was able to lower the room temperature by few degrees. It could be expected that with proper improvements such as a better material with thermal conductivity near to that of soil, proper insulation and sufficient ground depth would improve the performance of geothermal air cooling system.

TABLE OF CONTENTS

DECLARATION	iii
APPROVAL FOR SUBMISSION	iv
ACKNOWLEDGEMENTS	vii
ABSTRACT	viii
TABLE OF CONTENTS	ix
LIST OF TABLES	xii
LIST OF FIGURES	xv
LIST OF SYMBOLS / ABBREVIATIONS	xvii
LIST OF APPENDICES	xix

CHAPTER

1	INTRODUCTION	1
	1.1 Background	1
	1.2 Geothermal Cooling System	3
	1.3 Problem Statement	4
	1.4 Aim and Objectives	5
2	LITERATURE REVIEW	6
	2.1 Existing Geothermal Systems	6
	2.2 Geothermal Piping Materials	7
	2.3 Geothermal Ground Loop Design	11
	2.4 Cooling Load Analysis	14
	2.5 Radiant Time Series (RTS) Method	15
3	METHODOLOGY	18
	3.1 Location of Experiment and Description	18
	3.2 Selection of Piping Materials	19

3.3	Schematics of Proposed Experimental Design	22
3.3.1	General Layout of Experimental Design	22
3.4	Actual Layout of Experimental Design	23
3.4.1	Digging Holes for Installations of Pipes of Different Materials	23
3.4.2	Inserting K-type Thermocouples Probes	26
3.4.3	Creating Air Flow within Piping	27
3.4.4	On-site Measuring and Recording	29
3.5	Schematics of Prototype Design	32
3.5.1	General Layout of Prototype Design	32
3.6	Actual Layout of Prototype Design	34
3.6.1	Digging Holes for Installation of Pipe	35
3.6.2	Inserting K-type Thermocouples Probes	36
3.6.3	On-site Measuring and Recording	37
3.7	Implementation of Cooling Load Analysis and Radiant Time Series (RTS) Method	37
3.7.1	Internal Load: People	37
3.7.2	Internal Load: Lighting	39
3.7.3	Internal Load: Equipment	39
3.7.4	External Loads: Heat Transfer Through Opaque Surfaces	40
3.7.5	External Loads: Heat Transfer Through Fenestration	44
3.7.6	Infiltration of Outdoor Air and Moisture Transfer	45
3.8	Formula for Geothermal Air Cooling System	45
3.8.1	Formula for Volume Flow Rate	45
3.8.2	Formula for Piping Materials	47
4	RESULTS AND DISCUSSION	50
4.1	Heat Transfer Performance of Different Piping Materials for Experimental Design	50
4.2	Cooling Load Analysis with Implementation of Radiant Time Series (RTS)	58

4.2.1	Internal Heat Loads by People, Lighting and Equipment	58
4.2.2	External Loads by Heat Transfer Through Opaque Surfaces	60
4.2.3	Summation of Internal Load and External Load to Obtain Peak Cooling Load	65
4.3	Selection of Piping Materials for Prototype System based on Minimum Length and Cost	66
4.4	Results of Geothermal Air Cooling System for Prototype Design	71
5	CONCLUSION AND RECOMMENDATIONS	80
5.1	Conclusion	80
5.2	Recommendations	81
	REFERENCES	83
	APPENDICES	85

LIST OF TABLES

TABLE	TITLE	PAGE
2.1	Comparison of COP Values (Cooling and Heating) (Lam and Wong, 2005)	8
3.1	Materials Properties of Selected Materials (Callister, 2007)	20
3.2	Price List of Pipes of Selected Materials	20
3.3	Specification of K-type Thermocouples	30
3.4	Parameters of House and Room	32
3.5	Representative Rates at Which Heat and Moisture Are Given Off by Human Beings in Different States of Activity (ASHRAE, 2009)	38
3.6	Recommended Radiative/Convective Splits for Internal Heat Gains (ASHRAE, 2009)	38
3.7	Lighting Heat Gain Parameters for Typical Operating Conditions (ASHRAE, 2009)	39
3.8	Recommended Heat Gain from Typical Computer Equipment (ASHRAE, 2009)	40
3.9	Cooling Load Temperature Differences for Calculating Cooling Load from Sunlit Roof (ASHRAE, 1997)	41
3.10	Overall Heat Transfer Coefficient of Roof Type (Spitler, Jeffrey and Fisher, 1999)	43
3.11	Cooling Load Temperature Differences for Calculating Cooling Load from Sunlit Wall (ASHRAE, 1997)	43

3.12	Overall Heat Transfer Coefficient of Wall Type (Spitler, Jeffrey and Fisher, 1999)	44
4.1	Average Inlet and Outlet Temperature of Piping Materials from 26 th of March, 2015 to 28 th of March, 2015	50
4.2	Velocity, Average Velocity and Mass Flow Rate of Air	51
4.3	Diameter and Length of Respective Pipe	52
4.4	Amount of Heat Transfer to the Soil	53
4.5	Thermal Conductivity of Materials	56
4.6	Total Amount of Heat Gain by Students, Fluorescent Lighting and Laptops	59
4.7	Recommended Radiative and Convective Fraction for Students, Fluorescent Lighting and Laptops	59
4.8	Internal Heat Loads Generated in terms of Radiant and Convective Portion	60
4.9	Inside Room Temperature from 8 am to 6 pm and Average Room Temperature Before Installation of Geothermal Air Cooling System	61
4.10	Surrounding Area Temperature of the House	62
4.11	Parameters of Roof	63
4.12	Average Cooling Load Temperature Difference for Wall	64
4.13	Parameters of Wall	64
4.14	Internal Loads, External Loads and Total Peak Cooling Load	66
4.15	Different Pipes Required Length	67
4.16	Total Price of Pipe for Respective Pipe	71
4.17	Average Temperature of Inlet of Pipe, Outlet of Pipe and 1.5 m Beneath the Ground	72
4.18	Hourly Temperature Difference and Heat Transfer Rate	74

4.19	Values of Important Parameters	75
4.20	Effect of Geothermal Air Cooling System on Tested Room	79

LIST OF FIGURES

FIGURE	TITLE	PAGE
1.1	Carbon Dioxide Emissions and Energy Use In Malaysia (PERKEM VIII, 2013)	2
1.2	Cooling and Heating of House During Summer and Winter	3
2.1	Geothermal Loop and Pit	7
2.2	Chassis Outlet Temperature Inside Outdoor (Yuping, Yuening and Jian, 2009)	9
2.3	The View of Ground Heat Exchangers Buried at 1 m and 2 m Depths	12
2.4	Profile of Outdoor Cabinet with GCS	13
2.5	The View of Ground Heat Exchanger Buried at 2 m Depth	14
2.6	Cooling Loads Involved in Residential Buildings (ASHRAE, 2009)	16
2.7	Thermal Storage Effect in Cooling Load from Lights (ASHRAE, 2009)	17
3.1	The Location of Geothermal Air Cooling System	18
3.2	Actual Layout of Experimental Design	23
3.3	Hoes, Pick Axe, White Scope and Wheel Barrow	24
3.4	U-shape Configuration of Piping System	25
3.5	Installation of Piping Material Under The Ground	25
3.6	Drilling Machine and 5.0 mm Diameter Drill Bit	26

3.7	Insertion of K-type Thermocouples Probes Into the Drilled Hole	27
3.8	Attachment of Vacuum Cleaner Hose into Reducer	28
3.9	Digital Anemometer	29
3.10	K-type Thermocouples	30
3.11	Digital Infrared Thermometer (TM-909 AL) with K-type Thermocouples	31
3.12	Measuring Temperature with K-type Thermocouples and Digital Infrared Thermometer (TM-909 AL)	32
3.13	Schematic Design of Piping Configuration for Prototype Design (SolidWorks)	33
3.14	Front View, Side View and Surrounding Area of the House	34
3.15	Open Window Area After Installation of Pipe	35
3.16	Installation of Piping System Under the Ground	36
4.1	High-density Polyethylene Pipe and Polyvinyl Chloride (PVC) pipe	57
4.2	Rate of Heat Transfer for Different Pipes	58
4.3	Inlet and Outlet Temperature of the Pipe at Respective Hour	72
4.4	Ground Temperature at 1.5 m Beneath Surface of Ground	73
4.5	Heat Transfer Rate with respect to Corresponding Hours	74

LIST OF SYMBOLS / ABBREVIATIONS

Q	heat load, W
U	overall heat transfer coefficient, W/K
A	heat transfer area of the surface, m ²
$Corr.CLTD$	corrected cooling load temperature difference, K
$CLTD$	cooling load temperature difference, K
t_r	inside temperature, K
t_m	mean outdoor temperature, K
t_m	mean temperature difference, K
T_{max}	maximum outdoor temperature, K
ΔT	daily temperature range, K
Q_{trans}	heat load, W
$A_{unshaded}$	overall heat transfer coefficient, W/K K
\dot{Q}	volume flow rate, m ³ /s
c_p	specific heat capacity of air, kJ/kg K
ρ	density of air, kg/m ³
Q_a	air flow rate/volume flow rate, m ³ /s
V	velocity of air, m/s
A	cross sectional area of pipe, m ²
$R_{conductive}$	conductive resistance of pipe per unit length, m K/W
D_o	outer diameter of pipe, m
D_i	inner diameter of pipe, m
L	length of pipe, m
k_p	thermal conductivity of polyvinyl chloride (PVC), W/m K
h_{air}	convective heat transfer coefficient, W/m ² K
Nu	Nusselt number
k_a	thermal conductivity of air, W/m K

f	friction factor
Re	Reynolds number
Pr	Prandtl number
\dot{m}	mass flow rate, kg/s
μ	dynamic viscosity, kg/m s
R_{total}	total resistance of pipe per unit length, m K/W
w	work consumed by the centrifugal fan, W
$SHGF_{max}$	solar heat gain factor
SC	shading coefficient
CLF	cooling load factor
COP	coefficient of performance
HVAC	heat, ventilation, air conditioning
GCS	geothermal cooling solution
GSHP	ground-source heat pump

LIST OF APPENDICES

APPENDIX	TITLE	PAGE
A	Gantt Chart	85
B	Tables for On-site Measurement of Temperature for Piping Materials	86

CHAPTER 1

INTRODUCTION

1.1 Background

Geothermal heating and cooling is not well known by the general public in Malaysia, even though it has several key advantages and is steadily gaining in popularity. In fact, more than one million earth-coupled heat pumps have been deployed in the United States. Each year, American homeowners installed more than 50,000 geothermal heat pumps and the total market for geothermal heat, ventilation, air conditioning (HVAC) in the United States will achieve an estimated 3.7 billion dollars for 2009 (Stella Group, 2009).

There are plenty of good reasons to invest in a geothermal system. Geothermal cooling system is exceedingly reliable, quiet, and efficient. There is no smoke or fumes created, as there is no combustion. A geothermal cooling system provides steady, even temperature and humidity control throughout the day and night, without the extreme blasts of hot or cold air associated with conventional equipment. It will save money in the long run. Generally, it is a good deal than competing technologies such as solar or wind (Egg Geothermal, 2011).

Geothermal cooling system also helps to reduce the use of fossil fuels. The population of Malaysia has raised from 25.6 million to approximately 28 million by the year 2010, with an annual growth rate of 2.4 %. With this population growth rate, the energy demand is expected to increase, since energy consumption is an integral part and is proportional to the economic development and total population of a

country. In order to cope with the increasing demand for energy, it is universally accepted that renewable energy would be a sensible option in the future. The fact that Malaysia is endowed with abundance of natural resources for renewable energy exploitation, the majority of all the major power stations in Malaysia are still using fossil fuels, such as oil, gas and coal to generate electricity. Tenaga Nasional Berhad (TNB) is the largest electricity utility company in the country with the largest generation capacity of 10,481 MW (Alam Cipta, 2006).

The utilization of geothermal cooling system may help to reduce carbon emissions as well. Nowadays, the development of the world economy have an enormous impact, particularly on the environment. Global warming has always been a topic of discussion among world leaders. Carbon dioxide emissions has been identified as the main contributor to global warming. Based on statistics of carbon dioxide production in 2007, Malaysia with an estimate of 29 million tonnes ranked 26th (0.66 %) from 215 countries in the world. In pursuit of national development and improving the living standards of population, economic activities and projects for economic development cannot be avoided. People used to ignore environmental problems arising from the implementation of economic activities and development projects. Negative effect of a highly contagious substance through economic development now is the carbon dioxide released. Carbon dioxide released through industrial activities and the use of energy such as fossil fuels. Figure 1.1 shows the carbon dioxide emissions and energy use in Malaysia (PERKEM VIII, 2013).

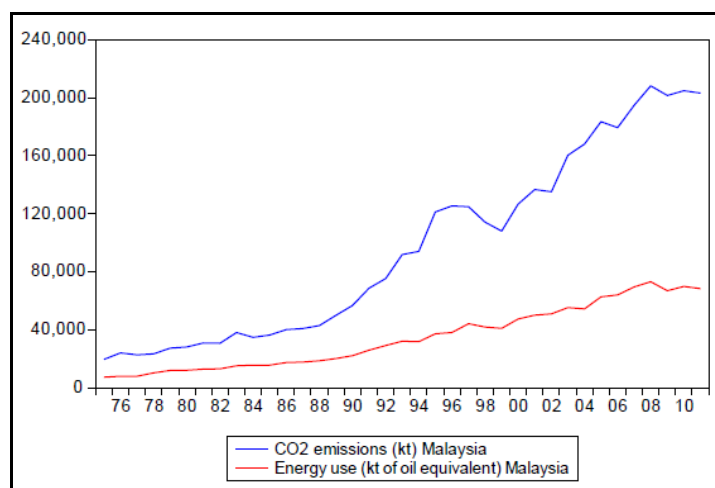


Figure 1.1: Carbon Dioxide Emissions and Energy Use In Malaysia (PERKEM VIII, 2013)

1.2 Geothermal Cooling System

The word “geothermal” has two parts, which are geo, meaning earth, and thermal, meaning heat. Thus, geothermal concerns using heat from the Earth. There are a few different applications of geothermal technology, however, the concern is now the implementation of geothermal cooling system in Malaysia. Geothermal cooling system is a shallow geothermal technology used to control the climate inside the buildings. “Shallow”, for our purposes, means not more than 500 feet below the surface. In United States, most geothermal climate systems do not go beyond this depth.

The geothermal cooling system takes the largely constant temperature of the earth for heating or cooling the home or business. During winter, the underground temperature is higher than ambient room temperature, therefore heating is required and the system draw heat energy from the Earth. During summer, it is a vice versa process. Figure 1.2(a) and Figure 1.2(b) show that geothermal cooling and heating using the relatively stable temperature of the earth to heat a building in the winter and cool it in the summer. This is called a ground source system because it uses the surrounding ground as a heat sink and a heat storage medium.

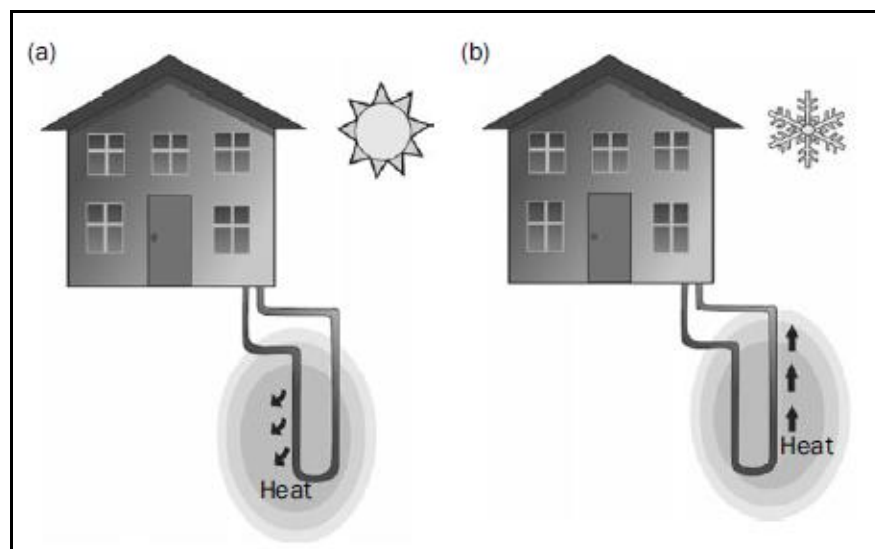


Figure 1.2: Cooling and Heating of House During Summer and Winter

Generally, there are two types of geothermal systems which are closed-loop geothermal and open-loop geothermal system. Closed-loop system uses a network of pipe buried underground to circulate water, air, refrigerant or anti-freeze solution from the ground to the heat pump. Closed loop systems are sealed and pressurised, with the fluid recirculating in the pipe, without causing any water usage. Closed-loop piping will last for more than 50 years if properly installed. Open-loop geothermal uses groundwater from a conventional well nearby the units as a heat source during winter or a heat sink during summer. The groundwater is pumped through the heat pump where heat is extracted during winter or rejected during summer, following the disposal of water in an appropriate manner. Groundwater is an excellent heat source or heat sink because it has a relatively constant temperature throughout the year (ClimateMaster, Inc., 2013).

1.3 Problem Statement

Various effort has been carried out to further amplify the advantages of implementing geothermal air cooling system in Malaysia as the fossil fuel demand is increasing in Malaysia while the supply of fossil fuel is becoming insufficient. This is where the implementation of renewable energy comes in. Solar energy is primarily the main renewable energy source in Malaysia. Therefore, there is room for growing demand of geothermal air cooling system in Malaysia as this system could attain a great cost savings and environmental friendly in a long run, and even the maintenance costs.

Therefore, in order to further amplify the advantages of implementing geothermal air cooling system in Malaysia, the first problem to be resolved in this project is the determination of suitable piping material for geothermal air cooling system. The piping material plays an important role in the geothermal air cooling process because the rate of heat transfer solely depends on the thermal conductivity of the piping material. The thermal conductivity of piping materials also strongly related to the thermal conductivity of soil. Besides that, different piping materials

may also vary in terms of cost. Therefore, a suitable piping material which has optimum thermal conductivity and great cost savings will be selected.

The second problem to be resolved is to determine the suitable ground loop design. Vertical loop geothermal air cooling system was greatly implemented in USA with depth up to 200 m. In order to achieve this depth, a special drilling technology is required. However, in Malaysia, this technology was so limited. Therefore, a horizontal ground loop system was implemented in this project. The piping configuration will be determined in order to minimize the area required for the installation of pipe, to ensure that the spacing between the pipes was sufficient enough, and to ease the installation process based on simple configuration and material saving issues.

The last problem to be resolved through this final year project was to study the coefficient of performance (COP) of geothermal air cooling system prototype built by using the selected piping material. It was believed that geothermal air cooling system can be used for cooling of residential and conventional buildings with an optimistic COP which we hope to obtain from our prototype system.

1.4 Aim and Objectives

In this research project, the main aim is to achieve temperature reduction in buildings by implementation of geothermal air cooling system in Malaysia using new piping materials. The research objectives in-line with the project are:

1. To determine the suitable piping material for increasing the efficiency of geothermal air cooling system.
2. To determine the most suitable piping material for prototype system by investigating the cost of pipe for the materials studied.
3. To study the coefficient of performance (COP) of geothermal air cooling system by using the selected piping material.

CHAPTER 2

LITERATURE REVIEW

2.1 Existing Geothermal Systems

American Journal of Engineering Research (AJER) (2013) presented a research paper on geothermal air conditioning in India. This research paper serves to provide interesting and important information of closed looped geothermal cooling system. The contents of the paper involves a brief description of geothermal air conditioning by necessary and descriptive images. Therefore, the basic working principle of geothermal cooling systems can be easily understand from this paper (Gaffar, 2013).

Geothermal air conditioning system works by harnessing energy from the Earth. The underground temperature remains constant below certain depth throughout the year irrespective of the ambient room temperature. In which, the underground temperature is higher and lower than the ambient room temperature during winter and summer season respectively. Consequently, there is an increase or decrease in the coefficient of performance (COP) or running efficient of all Heat, Ventilation, and Air Conditioning (HVAC) system (Gaffar, 2013).

The setup of geothermal air conditioning system consists of few major characteristics to be concerned of, which are, materials for earth-tube heat exchanger, earth-tube loop design, and contribution of the system to environment and economy of country. Figure 2.1 shows the horizontal earth-tube loop design where the network of pipes carrying refrigerant is being installed. The loop is usually installed in the moist soil to increase the efficiency of heat transfer between the refrigerant and earth.

At the depth of 2.5 m, the excavated soil shows the presence of moisture (Gaffar, 2013).

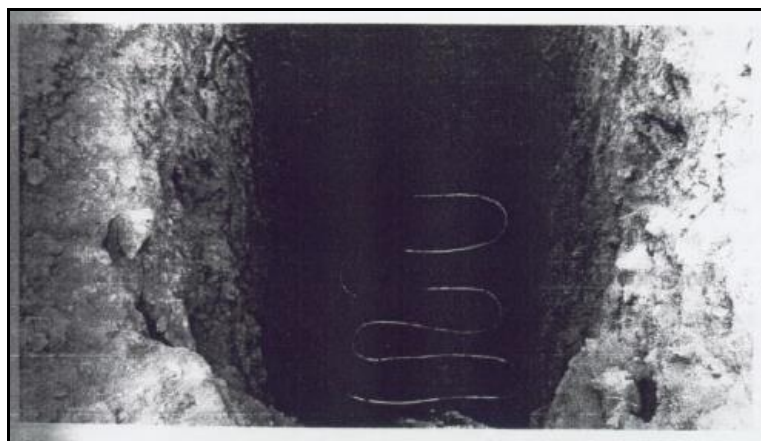


Figure 2.1: Geothermal Loop and Pit

Loop of 15 m long copper pipes with diameter of 12.5 mm were utilized in the closed loop system for circulating the refrigerant through the underground. Copper was selected for the purpose of cooling because it has a very high thermal conductivity of 380 W/m K. It also possessed a life time of up to 25 years. The daily maximum cooling coefficient of performance (COP) of the geothermal air conditioning system was noted to be 2.32 and the total average COP of the were calculated to be 2.12 (Gaffar, 2013).

2.2 Geothermal Piping Materials

In United States, the most widely used material for the installation of geothermal piping system is high-density polyethylene (HDPE) (Geothermal Heat Exchange Wells, 1999). The International Ground Source Heat Pump Association (IGSHPA) specifies that HDPE is suitable to be used for the geothermal piping system for either cooling or heating because of its excellent heat transfer property, chemically inert, flexible to be bend without kinking, long anticipated life span, and also has a high abrasion resistance.

Similarly, Hong Kong government has initiated a project for the Wet Land Garden in the New Territories in which geothermal system is installed for the purpose of cooling and heating of the associated buildings. Further analyses of the results can help to determine whether geothermal system are environmental friendly and economically viable to be implemented in Hong Kong. Vertical U-tube ground loop heat exchangers made of high-density polyethylene tubing were installed. High-density polyethylene is widely used because it has a thermal conductivity of 0.48 W/m K, which is lower than the thermal conductivity of ground layer which is 2.60 W/m K. This is a major concern so as to avoid the case of under-utilization. The coefficient of performance achieved are shown in the Table 2.1, which is in line with the heat pump manufacturer's rated COP of 3.2. Thus, it can be concluded that geothermal system is feasible for the purpose of heating and cooling of buildings in Hong Kong (Lam and Wong, 2005).

Table 2.1: Comparison of COP Values (Cooling and Heating) (Lam and Wong, 2005)

Year of Operation	COP
1 st year	3.29
6 th year	3.20
17 th year	3.25

In China, the utilization of geothermal cooling solution for outdoor cabinets used to contain telecom equipment are being researched. The water-soil exchanger made of high-density polyethylene material tube is buried 2.4 m depth underground. Anti-corrosive and high reliable high-density polyethylene is widely used in geothermal system. When geothermal cooling solution is applied, the air temperature in the outdoor cabinet was able to decrease by a maximum amount of 25 °C, achieving COP of 34, which is much higher than conventional cooling method (Yuping, Yuening and Jian, 2009). Figure 2.2 shows the chassis outlet temperature for outdoor cabinets.

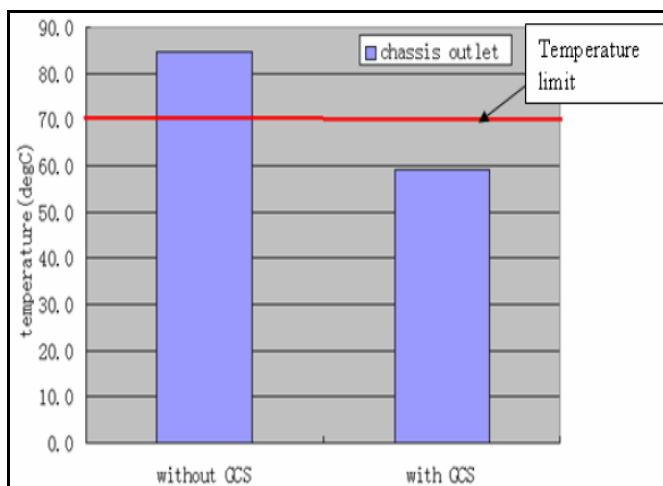


Figure 2.2: Chassis Outlet Temperature Inside Outdoor (Yuping, Yuening and Jian, 2009)

In India, space heating and cooling account for about 30 % of total energy consumption. Geothermal energy is an effective alternative cooling system for cooling of buildings to decrease the energy consumption. The summer cooled building using geothermal unit consists of series of underground piping system made of galvanized iron heat exchange was carried out. Geothermal cooling system consumed less energy compared to conventional air conditional because it uses water as the transporting fluid in the piping which enable the transfer of heat to be more efficient due to higher specific heat capacity of water. Besides that, geothermal cooling system is very efficient and economically viable to be used for cooling of buildings. The maximum saving in terms of energy and values are obtained in May because maximum heat gain occurred on that month. The maximum savings are 692 kWh in terms of energy while RM 195.60 in terms of value (Pal, 2013).

The demand for energy is increasing and causes depletion of fossil fuels, leading the world to face the steady rise in the cost of electricity and conventional fuels. Consequently, influencing some country, such as India, to seek for alternative energy which is renewable energy, one of which is geothermal energy. Geothermal energy is found to be efficient as well for heating and cooling of water. This geothermal heating or cooling system has high thermal efficiency since no conversion of energy is required. The heat exchanger being installed underground is made of galvanized iron pipe with thermal conductivity of 53.3 W/m K. An

geothermal water tank is also being installed 3 m depth underground to store water at moderate temperature for normal use. The task of this geothermal system is to bring the water temperature from 6 °C and 48 °C during winter and summer respectively to 28 °C. The geothermal heat energy harnessed in the Earth could be able to heat and cool the water to the temperature which is suitable for normal use. Upon completion of task, this system was found to be efficient, at the same time, achieving savings both in terms of value and energy. The corresponding savings in terms of value are RM 409.90 for heating and RM 179.50 for cooling. The energy saving for heating during winter season is 1569 kWh and that for cooling during summer season is 687 kWh (Pal, 2013).

Malaysia is a tropical country where temperature escalates during daytime and goes beyond to a comfortable limit. Implementation of geothermal cooling system also being carried out by using aluminium as the pipe material. Aluminium is considered as high thermal conductivity material among metals. This can be proved by examining the performance of the aluminium in transferring the heat from room to the underground soil, making the cooling of building effectively. Numerical study on the heat transfer for cooling of residential low rise building was found to be possible by installation of high thermal conductivity pipes such as aluminium in connection with the underground soil where temperature remains constant and less than the ambient room temperature. From the analysis, it can be seen that square shaped aluminium pipes are effective in rejecting the heat to the underground soil with a temperature drop of 2.8 °C (Alam, Zain and Kaish, 2012).

The material of pipe for geothermal applications can be polyvinyl chloride (PVC) as well. Polyvinyl chloride (PVC) is a very common and widely used non-metallic pipe because of its acceptable service life. The piping system of geothermal air cooling system should be constructed with material which is strong, durable, corrosion-resistance, and also cost effective such as polyvinyl chloride (PVC). A fact proved by U.S. Department of Energy (USDOE), the thermal performance of a geothermal air cooling system has little influence by the choice of material. However, the thermal conductivity of material should near to the thermal conductivity of soil and thermal resistance should be as low as possible. Wale and Attar (2013) proposed the use of polyvinyl chloride (PVC) pipe as the piping system because polyvinyl

chloride was believed to be more prone to bacterial growth than other materials. According to Wale and Attar (2013), polyvinyl chloride pipe should be buried at least 1.8 m deep and placed in shady locations. Typically, the diameter of the pipe for geothermal air cooling system ranging from 150 mm to 500 mm will permit a greater airflow. Although smaller diameters are preferred for a better rate of heat transfer, but a smaller diameters will generate a higher friction losses. Lastly, a 100 mm diameter of polyvinyl chloride (PVC) pipe was used. After implementation of geothermal air cooling system, the energy used for cooling is reduced by 1.56 kWh per day and cost saving of RM 19.40 per month during summer days. Besides that, the temperature inside the building was able to reduce by 1.62 °C.

2.3 Geothermal Ground Loop Design

Mustafa Inalli and Hikmet Esen carried out the experiment to validate the performance of horizontal loop ground-source heat pump (GSHP) system used for space heating. An experiment room with 16.24 m² of floor area was designed and constructed in Firat University, Elazig, Turkey and connected to the GSHP system. The heating and cooling load of the experiment room was found to be 2.5 kW and 3.1 kW at the design conditions respectively. During heating season of year 2002 to 2003, the experimental results were collected from November to April. It was found that the average COP of the system for horizontal ground heat exchanger in different trenches with depth of 1 m and 2m were 2.66 and 2.81 respectively. From the results obtained, Mustafa Inalli and Hikmet Esen concluded that the horizontal loop ground-source heat pump system was feasible for Elazig, Turkey climatic conditions (Inali and Esen, 2004). Figure 2.3 shows the view of ground heat exchangers buried at 1 m and 2 m depth.



Figure 2.3: The View of Ground Heat Exchangers Buried at 1 m and 2 m Depths

Yuping Hong, Yuening Li and Jian Shi presented their ongoing research on geothermal cooling solution for outdoor cabinets that are used to contain telecom equipment such as FTTX network, mobile network and etc. The working principle of GCS system is that the heat generated by the telecom equipment is being dissipated from the water to the shallow underground soil by water-soil heat exchanger. The water-soil heat exchanger is made up of horizontal looping, that consists of three layers with depth of 1.2 m, 1.8 m and 2.4 m respectively. Compared with vertical looping, horizontal looping is easier to install because vertical looping requires special drilling machine and takes more time and money. The GCS system was able to decrease the maximum air temperature of the outdoor cabinet by 25 °C (85 °C to 60 °C), resulting in COP of 34, which is much more higher than traditional air conditioning system (Yuping, Yuening and Jian, 2009). Figure 2.4 shows the profile of outdoor cabinet with GCS.

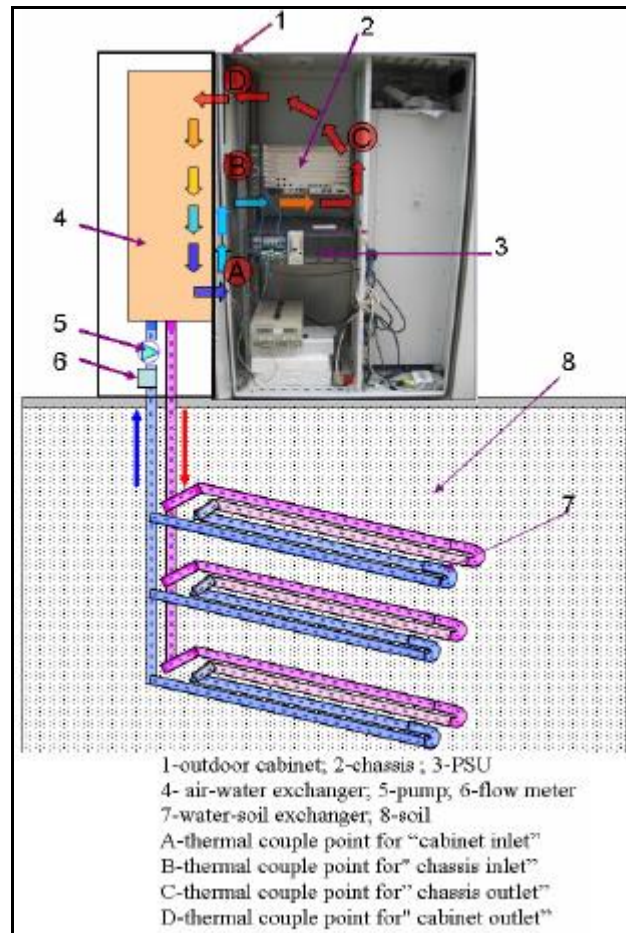


Figure 2.4: Profile of Outdoor Cabinet with GCS

Wale and Attar (2013) proposed that horizontal closed loop with parallel connections are generally most cost-effective for small installations, particularly for new construction where only sufficient land area is available. The results were obtained in 2013 with ventilation system being turned on and shows a positive feedback. The design was installed in Magar, Kolhapur, and was able to reduce the room temperature by 1.62 °C (Pravin and Attar, 2013). Figure 2.5 shows the view of ground heat exchanger buried at 2 m depth.



Figure 2.5: The View of Ground Heat Exchanger Buried at 2 m Depth

2.4 Cooling Load Analysis

Thermal load is the amount of heat that must be removed from the space to maintain a proper temperature in the space. When thermal loads push conditions outside of the comfort range, HVAC systems play an important role in bringing the thermal conditions back to comfort conditions (Dossat and Horan, 2002).

Cooling load is a very important parameter for warm climate and summer design, like in Malaysia. The heat transfer mechanism involved conduction, convection and radiation. Cooling load analysis is an important analysis for estimating the required capacity cooling systems for maintaining the required conditions in the conditioned space. To do so, information on the design indoor and outdoor conditions, specifications of the conditioned space, specifications of the building and any special requirements of the particular application must be required.

For comfort applications, the required indoor conditions are fixed by the criterion of thermal comfort. For industrial or commercial applications, the required indoor conditions are fixed by the particular processes being performed or the products being stored (Dossat and Horan, 2002).

In a nutshell, in order to study the cooling load required for a building, thermal properties of building materials are very important, which are overall thermal transmittance (U-value), thermal conductivity of the building materials and thermal capacity (specific heat) of building materials. In effort of determining the overall heat gain of a building and eventually the cooling load analysis, building survey for thermal loads estimation have to be identified as well, which are orientation of the building, use of spaces, physical dimensions of spaces (ceiling height, columns and beams), construction materials, surrounding conditions, windows, doors, stairways, people (number of density, duration of occupancy, nature of activity), lightning, appliances, ventilation, thermal storage (if any) and continuous or intermittent operation (Dossat and Horan, 2002).

2.5 Radiant Time Series (RTS) Method

Cooling load is the amount of heat that must be removed from the space to maintain the proper temperature in the space (Dossat and Horan, 2002). The radiant time series (RTS) method can be implemented together with cooling load analysis to simplify the calculation of cooling load.

Cooling load can be categorised into external loads and internal loads. External loads involved the heat gain through exterior walls and roofs, solar heat gain through fenestrations (windows), conductive heat gain through fenestrations, heat gain through partitions and interior doors, and infiltration of outdoor air. Internal loads involved people, electric lights, equipment and appliances, sensible cooling loads and latent cooling loads. Figure 2.6 shows the cooling loads involved in a residential building. Besides that, cooling load analysis also had to take into account the effect of heat storage. Figure 2.7 shows the thermal storage effect in cooling load

from lights. Therefore, when performing the calculation of cooling loads, has to consider the unsteady state processes, as the peak cooling load occurs during the day time and the outside conditions vary significantly throughout the day due to solar radiation. In addition, all internal sources add on to the cooling loads and neglecting them would lead to underestimation of the required cooling capacity and the possibility of not being able to maintain the required indoor conditions (Dossat and Horan, 2002).

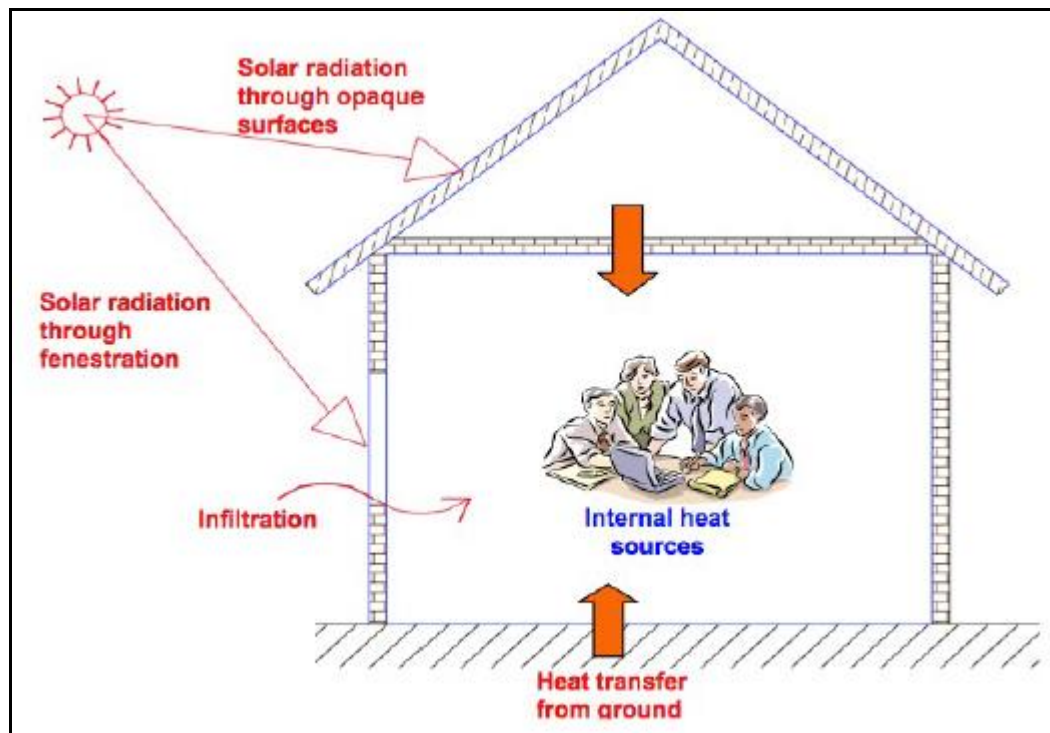


Figure 2.6: Cooling Loads Involved in Residential Buildings (ASHRAE, 2009)

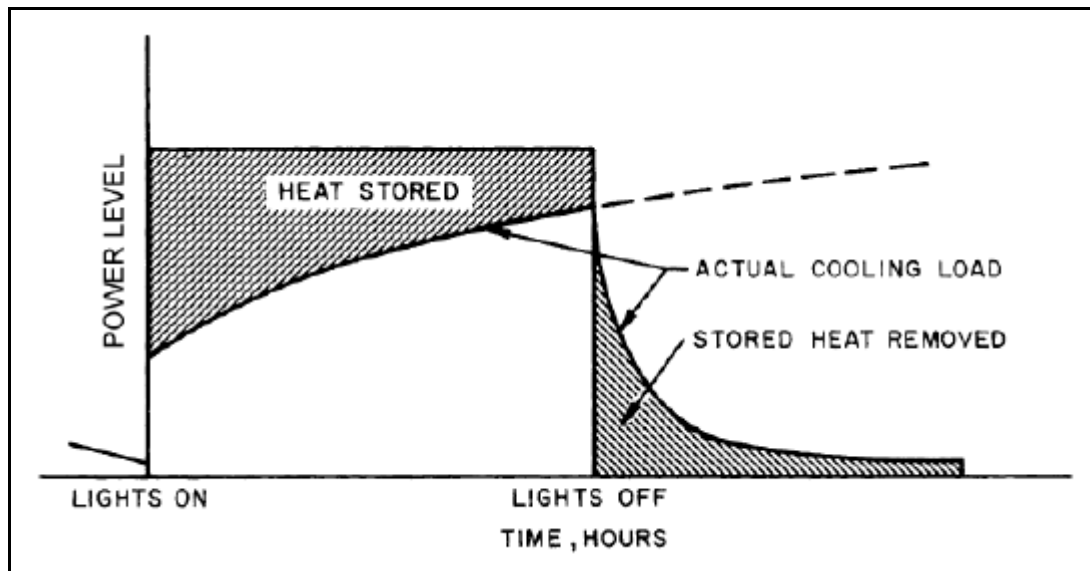


Figure 2.7: Thermal Storage Effect in Cooling Load from Lights (ASHRAE, 2009)

Since cooling load calculations must take into account the time-delay effects occurring during the heat transfer process across the building. Radiant time series (RTS) is a simplified method that is demanding and does not require any iterative calculation. Radiant time series (RTS) take into consideration the time delay effect of heat energy in which the surface of the building or within the building itself experienced (ASHRAE, 2009).

CHAPTER 3

METHODOLOGY

3.1 Location of Experiment and Description

The geothermal cooling system is located within UTAR Setapak which is shown in Figure 3.1.



Figure 3.1: The Location of Geothermal Air Cooling System

3.2 Selection of Piping Materials

The three major factors that determine the selection of pipe material for the prototype design of geothermal air cooling system are listed below:

1. The thermal conductivity, k of the material
2. The cost of material
3. The availability of each material in the market

In this project, four types of pipes of different materials have been reviewed from the journal to identify their suitability for geothermal piping system. The pipes of different materials were compared based on the three factors listed. The four different materials being studied are:

1. High-density polyethylene pipe (HDPE)
2. Galvanized Iron
3. Aluminium
4. Polyvinyl Chloride (PVC)

Table 3.1 shows the details of each material with respect to their properties while Table 3.2 shows the price list of the pipes of different material available in the marketplace. The price list was obtained from the hardware vendors in Kuala Lumpur.

Table 3.1: Materials Properties of Selected Materials (Callister, 2007)

Material	Properties			
	Thermal conductivity, k (W/m K)	Density, γ (g/cm ³)	Yield Strength, F_y (MPa)	Young's Modules, E (GPa)
High-density polyethylene (HDPE)	0.48	0.959	26.2 – 33.1	1.08
Galvanized Iron	53.3	7.85	195	13.4
Aluminium	222	2.71	34	69
Polyvinyl Chloride (PVC)	0.15 – 0.21	1.30 – 1.58	12 – 43	2.41 – 4.14

Table 3.2: Price List of Pipes of Selected Materials

Material	Galvanized Iron	PVC	Aluminium	HDPE
Price Per Meter at 20 mm Outer Diameter (in RM)	7.33	2.67	8.23	1.08

*Note: All price lists are as per current market listing of material at Year 2015 (may subject to change)

By comparing the data of the four materials obtained, polyvinyl chloride (PVC) was selected to be the piping material for the geothermal air cooling system. First of all, by comparing the thermal conductivity of polyvinyl chloride (PVC) to that of aluminium, although aluminium pipe has a much higher thermal conductivity than polyvinyl chloride (PVC), which is 222 W/m K. However, this doesn't mean that the material is suitable to be used in geothermal air cooling system. The soil thermal conductivity is around 0.45 W/m K at maximum moisture content (Din, 2011). Aluminium may be under-utilized. In other words, heat accumulation would occur if the rate of heat rejection from the pipe to the soil is higher than the rate in which the soil is capable of conducting the heat away to the earth reservoir. Consequently, the soil temperature around the pipe will increase and heat up the pipe,

which in turn, in the long run, the temperature at the outlet of the pipe would increase, which should be avoided. The main reason polyvinyl chloride (PVC) was chosen over aluminium was because of its relatively low cost as well. Therefore, aluminium pipe was not taken into consideration.

Polyvinyl chloride (PVC) pipe is preferable over galvanized iron because of the inertness and stability of polyvinyl chloride (PVC). Galvanized pipes are generally replaced rather than repaired because they are difficult to repair. When galvanized pipes get damaged, the zinc later of the galvanization will get weaker and consequently will start to corrode in a short period of time. For a geothermal air cooling system, it was preferable to have a low maintenance cost or less maintenance require, therefore polyvinyl chloride (PVC) plays a vital role in this point of view. When compared to galvanized iron pipe, polyvinyl chloride (PVC) pipe are not that expensive as well. Besides that, galvanized iron pipes are heavy to handle because they are made up of iron and steel. The main reason polyvinyl chloride (PVC) was chosen over galvanized iron because of its relatively low cost as well. Therefore, galvanized iron pipe was not taken into consideration.

Although high-density polyethylene (HDPE) has the material properties better than polyvinyl chloride (PVC), polyvinyl chloride is better in term of formability. High-density polyethylene (HDPE) is difficult to form into straight line as compared to polyvinyl chloride (PVC), which may cause trouble during installation of piping system. Besides that, although high-density polyethylene has a slightly higher thermal conductivity than polyvinyl chloride (PVC) pipe and also has a nearest thermal conductivity to the soil. These factors can be compensated by the thickness of polyvinyl chloride (PVC) pipe. The thickness of polyvinyl chloride (PVC) pipe is smaller as compared to high-density polyethylene (HDPE) pipe, this may improve and also balance the rate of heat transfer to the soil.

An experiment was constructed to identify the performance of high-density polyethylene (HDPE) pipe, galvanized iron pipe, aluminium pipe and polyvinyl chloride (PVC) pipe. The different materials of pipes with equal length and equal diameter were obtained from the hardware shop. By passing air through the four different pipes, a K-type thermocouple was used to measure the temperature at the

inlet and outlet of the pipe. The results obtained were analysed and compared. The highest temperature difference between the inlet and outlet pipe indicates the suitable material to be implemented in geothermal air cooling system.

3.3 Schematics of Proposed Experimental Design

The selection of the pipe to be used in the geothermal air cooling system was done by comparing the material properties and also the cost of the pipes in section 3.2. Before finalize the design of the prototype, a small scale experimental design that has been scale down by 30 % was conducted for further studies on the selection of piping materials. The schematics of proposed experimental design was divided into two sections. The first section shows the general layout of experimental design. The second section shows the piping schematics of the pipes buried under the earth at the desired depth.

3.3.1 General Layout of Experimental Design

In the selection of piping materials section, four types of pipes which are HDPE, galvanized iron, aluminium and PVC were buried at a depth of 1.5 m underground. The length of the pipes was constructed to be 2.5 m with 1.5 m buried under earth and 1 m exposed above the ground. The experimental setup generally consists of two sections.

The first section is the inlet of the four types of pipes. Atmospheric air was being sucked into the pipes by using vacuum cleaner. The second section is the outlet of the four types of pipes. Atmospheric air was passed over the pipe by using the vacuum cleaner to force the atmospheric air channel into the piping system. A reducer was installed at the outlet of the pipe to prevent air from leaking into the atmosphere, at the same time, to create sufficient air velocity.

3.4 Actual Layout of Experimental Design

The actual layout of experimental design was constructed as shown in Figure 3.2. The setup of experimental design was divided into four sections. The first section is digging holes for installations of pipes of different materials. The second section is inserting K-type thermocouples probes. The third section is creating air flow within the pipes. The fourth section is on-site measuring and recording of temperature at the inlet and outlet of pipes.



Figure 3.2: Actual Layout of Experimental Design

3.4.1 Digging Holes for Installations of Pipes of Different Materials

The digging of holes to bury the four types of pipes at 0.5 m below the ground was done by using hoes, pick axe, white scope and a wheel barrow.

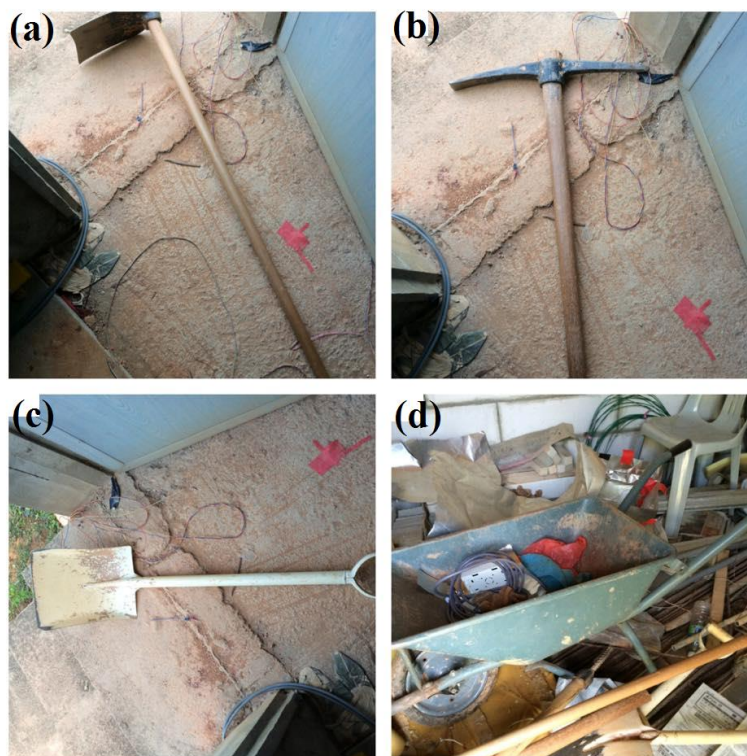


Figure 3.3: Hoes, Pick Axe, White Scope and Wheel Barrow

It took approximately 2 days to bury the required area for installation of four types of pipes which were installed 0.5 m below the ground. Each type of pipes was connected by using two 90° elbows of respective materials. Figure 3.4 shows four types of pipes of different materials. On the top left corner of Figure 3.4 is the high-density polyethylene (HDPE) pipe. On the top right corner of Figure 3.4 is the aluminium pipe. The bottom left corner of the figure shows the polyvinyl chloride (PVC) pipe. The galvanized iron pipe is on the bottom right corner of the figure.



Figure 3.4: U-shape Configuration of Piping System

After the assembly of four types of pipes, the pipes are buried into the area of ground with depth of 0.5 m. Figure 3.5 shows the process of installation of piping material under the ground.



Figure 3.5: Installation of Piping Material Under The Ground

3.4.2 Inserting K-type Thermocouples Probes

Following the installation of piping system under the ground, K-type thermocouples probes was inserted. The temperature of the air at the inlet and outlet of the pipes were recorded and analysed.

In order to measure the temperature of the air within the pipe, a hole was drilled on the body of the pipe. Before the setup of piping systems, the pipes were brought to mechanical workshop. The drilling machine in the mechanical workshop was used with a 5.0 mm diameter drill bit to drill holes on the indicated mark on the pipe. Figure 3.6 shows the drilling machine and 5.0 mm diameter drill bit.



Figure 3.6: Drilling Machine and 5.0 mm Diameter Drill Bit

K-type thermocouples probes were inserted into the drilled hole to measure the temperature of the air, while the other end of the K-type thermocouples was attached to the digital infrared thermometer (TM-909 AL). Figure 3.7 shows the

insertion of K-type thermocouples probes into the drilled hole on the galvanized iron pipe for both inlet and outlet of the pipe.



Figure 3.7: Insertion of K-type Thermocouples Probes Into the Drilled Hole

3.4.3 Creating Air Flow within Piping

In the experimental design, four types of the pipes whereby galvanized iron pipe, polyvinyl chloride (PVC) pipe, aluminium pipe and high-density polyethylene (HDPE) pipe were buried at a depth of 0.5 m. The length of the pipes was constructed to be 1.5 m covered with the soil. Atmospheric air was then channelled at one end of each pipe. The temperature at inlet and outlet of the pipe were measured and compared.

PENSONIC PVC-22B vacuum cleaner was used to channel the air into each pipe. Vacuum cleaner was selected to suck the air into the pipe instead of hair dryer because vacuum cleaner was able to produce a constant air flow across the pipe. Besides that, the vacuum cleaner sucked in the atmospheric air at the atmosphere

temperature, which is much more make sense as what the prototype design did. If using hair dryer, the hair dryer was producing hot air at temperature higher than atmosphere temperature, which is not relevant to our system as it is impossible for atmosphere temperature to heat up to 50 °C plus in Malaysia. Besides that, a reducer was made using aluminium foil to prevent air from leaking into the atmosphere and also to create sufficient air velocity. Figure 3.8 shows the hose of vacuum cleaner inserted into the reducer at the pipe outlet.



Figure 3.8: Attachment of Vacuum Cleaner Hose into Reducer

The velocity of the air at the inlet and outlet of the pipes were measured by using digital anemometer provided. Figure 3.9 shows the digital anemometer provided.



Figure 3.9: Digital Anemometer

3.4.4 On-site Measuring and Recording

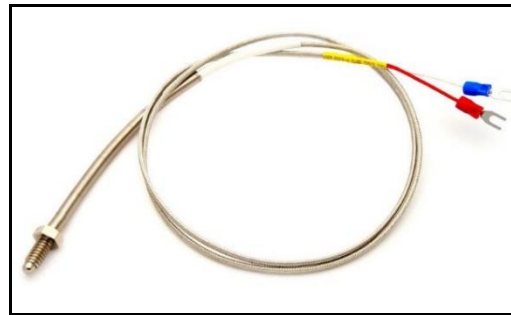
The measurement of temperature was carried out using K-type thermocouples and digital infrared thermometer (TM-909 AL). The thermocouple was connected to the digital infrared thermometer with the K-type thermocouples insertion slots on it.

The K-type thermocouples is a temperature sensor which was selected as the temperature measuring equipment for measuring the temperature. K-type thermocouples consists of two wire legs welded together to form a junction. This junction measured the temperature by creating a voltage difference. The two wire legs of K-type thermocouples are made of two dissimilar metals which are nickel-chromium alloy as the positive terminal and nickel-alumel alloy as the negative terminal. Table 3.3 shows the specification of K-type Thermocouples.

Table 3.3: Specification of K-type Thermocouples

Description	Specifications
Cable Length	2 m
Probe Length	9/16 inches
Thread	1/4 – 20
Temperature Range	-200 °C to 1250 °C

K-type thermocouples was selected to measure the temperature throughout the experiment because it is inexpensive, reliable, accurate, has a wide range of temperature and easy to obtain from the market. Figure 3.10 shows the K-type thermocouples that was being used in the experiment.

**Figure 3.10: K-type Thermocouples**

The temperature of the concerned objects can be measured by attaching the hot junction of thermocouple to them until thermal equilibrium is achieved. The temperature difference between the hot junction and cold junction generates a small potential difference. This signal is received by the digital infrared thermometer (TM-909 AL). The digital infrared thermometer will convert the potential difference readings into temperature readings through transfer function and display on the screen. Several precautions must be taken in order to attain high accuracy. One of which is short period of time must be allowed for the cold junction plugs of K-Type thermocouples to stabilize at the temperature of the sockets which are in direct contact with the built-in cold junction compensation. Figure 3.11 shows the digital infrared thermometer (TM-909 AL) with K-type thermocouples attached on it.



Figure 3.11: Digital Infrared Thermometer (TM-909 AL) with K-type Thermocouples

After the K-type thermocouples has been inserted into the drilled hole on the pipe, the measurement of temperature at both inlet and outlet of the pipe were being carried out. The measurement started from 10.30 am to 5.30 pm, with one hour interval between the measurements. The temperature was measured by inserting the probes of K-type thermocouples into the drilled hole on the pipe, while the other end of K-type thermocouples was attached to the digital infrared thermometer (TM-909 AL).

The power of vacuum cleaner was turned on to allow the air to channel into the pipe for 5 minutes before the temperature was measured and recorded. The result has been tabulated and discussed in Chapter 4. Figure 3.12 shows the measuring of temperature with K-type thermocouples and digital infrared thermometer (TM-909 AL).



Figure 3.12: Measuring Temperature with K-type Thermocouples and Digital Infrared Thermometer (TM-909 AL)

3.5 Schematics of Prototype Design

The schematics of prototype design is produced by using SolidWorks. Before producing the schematics diagram from SolidWorks. The house and room parameters were obtained.

3.5.1 General Layout of Prototype Design

The dimensions of the house as well as room was shown in Table 3.4

Table 3.4: Parameters of House and Room

Parameters	Length, l (m)	Width, w (m)	Height, h (m)
House	9.25	4.72	5.23
Room	2.97	4.47	3.23

The prototype system consists of two different sections, which are general layout of the geothermal air cooling system above the ground and also the piping configuration of the pipes buried under the earth at desired depth.

The first section consists mainly of the inlet of the pipe into the ground and the outlet of the pipe coming out from the ground. The inlet channel was connected to the room to channel the hot air from the room into the pipes. The outlet channel was connected to an exhaust fan to force the air into the piping system and channel back to the room after passing through the returning pipes under the ground. This section also consists of the insulation material for the part of the pipes which was exposed to sunlight during daytime.

The second section was the piping configuration at desired depth. This section consists mainly of ground heat exchanger which is the geothermal piping system. The geothermal pipes was placed at a depth of 1.5 m from the ground. The heat transfer between the ground and the pipe occurs in this section of the geothermal air cooling system. Figure 3.13 shows the schematic design of piping configurations for prototype design.

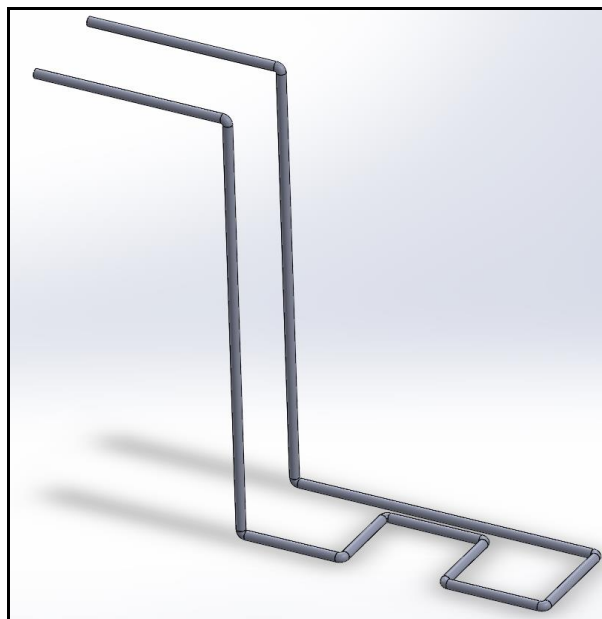


Figure 3.13: Schematic Design of Piping Configuration for Prototype Design (SolidWorks)

3.6 Actual Layout of Prototype Design

The prototype for the geothermal air cooling system was installed in one of the rooms in a house which was located within University Tunku Abdul Rahman. The house consists of three rooms and the house is made of light weight concrete material. The room which has been selected for carrying out the project consists of a plastic door and an open window area. Figure 3.15 shows the front view, side view and surrounding area of the house.



Figure 3.14: Front View, Side View and Surrounding Area of the House

The open window area was sealed with plywood and has two openings. The openings were located below the two corner of the open window area in order to reduce the length of the piping system exposed to sunlight, at the same time, may help to save material. The first opening located at the bottom left of open window area was the inlet of the piping system. The second opening located at the bottom right of open window area was the outlet of the piping system. This opening was connected to an exhaust fan to force the hot air into the piping system and channel the cooled air back to the room. The first opening was labelled as inlet while the second opening was labelled as outlet. Figure 3.15 illustrates the inlet and outlet of the piping system after the installation.

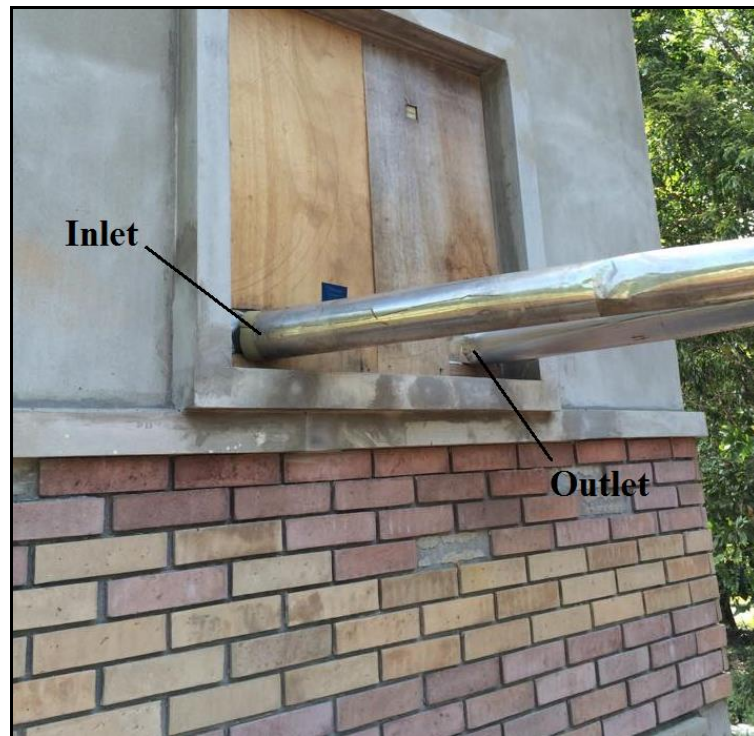


Figure 3.15: Open Window Area After Installation of Pipe

3.6.1 Digging Holes for Installation of Pipe

The digging of holes for installation of piping system was carried out by using hoes, pick axe, white scope and a wheel barrow.

It took approximately two weeks to bury the required area for the installation of piping system which were 1.5 m below the ground. The piping system were installed in a horizontal arrangement with the piping configuration shown in Figure 3.16. The piping system was installed based on the following criteria,

1. To minimize the area required for the installation of pipe
2. To ensure that the spacing between the pipes was sufficient enough to prevent heat dispersed being absorbed by the neighbouring pipe to ensure efficient cooling effect.
3. To ease the installation process based on simple configuration and material saving issues.

Figure 3.16 shows the piping system for the prototype design.



Figure 3.16: Installation of Piping System Under the Ground

3.6.2 Inserting K-type Thermocouples Probes

Following the installation of piping system under the ground, K-type thermocouples probes was inserted. The temperature of the air at the inlet and outlet of pipe were recorded and analysed.

In order to measure the temperature of the air within the pipe, a hole was drilled on the pipe. The hole was drilled by using BOSCH hand drill and 5.0 mm drill bit which were borrowed from UTAR mechanical workshop. After the hole was drilled, K-type thermocouples probes were inserted into the drilled hole for measuring the temperature of the air, while the other end of the K-type thermocouples is attached to the digital infrared thermometer (TM-909 AL). After the insertion, the K-type thermocouples probes was covered with dark tape to prevent the air leaking out from the pipe.

3.6.3 On-site Measuring and Recording

After the K-type thermocouples has been inserted into the drilled hole on the pipe, the measurement of temperature at inlet and outlet of the pipe were being carried out. The measurement was carried out from 8.00 am to 6.00 pm, with one hour interval between the measurements. An exhaust fan was turned on to allow the air to channel into the pipe for throughout the day.

3.7 Implementation of Cooling Load Analysis and Radiant Time Series (RTS) Method

3.7.1 Internal Load: People

For the internal heat load generated by people, it has been assumed that the room would occupied with two students throughout the day.

By referring to Table 3.5, the heat load generated by one student is 245 Btu/h which is 70 W. Assuming that both the two student will be seated and doing light work, the total internal heat load generated by the two student would be 140 W.

With the implementation of radiant time series (RTS) method, the constant hourly heat gain would be categorised into convective portions and also radiant portions by using the coefficients provided in Table 3.6.

Table 3.5: Representative Rates at Which Heat and Moisture Are Given Off by Human Beings in Different States of Activity (ASHRAE, 2009)

Degree of Activity	Location	Total Heat, Btu/h		Sensible Heat, Btu/h	Latent Heat, Btu/h	% Sensible Heat that is Radiant ^b	
		Adult Male	Adjusted, M/F ^a			Low <i>V</i>	High <i>V</i>
Seated at theater	Theater, matinee	390	330	225	105		
Seated at theater, night	Theater, night	390	350	245	105	60	27
Seated, very light work	Offices, hotels, apartments	450	400	245	155		
Moderately active office work	Offices, hotels, apartments	475	450	250	200		
Standing, light work; walking	Department store; retail store	550	450	250	200	58	38
Walking, standing	Drug store, bank	550	500	250	250		
Sedentary work	Restaurant ^c	490	550	275	275		
Light bench work	Factory	800	750	275	475		
Moderate dancing	Dance hall	900	850	305	545	49	35
Walking 3 mph; light machine work	Factory	1000	1000	375	625		
Bowling ^d	Bowling alley	1500	1450	580	870		
Heavy work	Factory	1500	1450	580	870	54	19
Heavy machine work; lifting	Factory	1600	1600	635	965		
Athletics	Gymnasium	2000	1800	710	1090		

Notes:

1. Tabulated values are based on 75°F room dry-bulb temperature. For 80°F room dry bulb, total heat remains the same, but sensible heat values should be decreased by approximately 20%, and latent heat values increased accordingly.

2. Also see Table 4, Chapter 9, for additional rates of metabolic heat generation.

3. All values are rounded to nearest 5 Btu/h.

^aAdjusted heat gain is based on normal percentage of men, women, and children for the application listed, and assumes that gain from an adult female is

85% of that for an adult male, and gain from a child is 75% of that for an adult male.

^bValues approximated from data in Table 6, Chapter 9, where *V* is air velocity with limits shown in that table.

^cAdjusted heat gain includes 60 Btu/h for food per individual (30 Btu/h sensible and 30 Btu/h latent).

^dFigure one person per alley actually bowling, and all others as sitting (400 Btu/h) or standing or walking slowly (550 Btu/h).

Table 3.6: Recommended Radiative/Convective Splits for Internal Heat Gains (ASHRAE, 2009)

Heat Gain Type	Recommended Radiative Fraction	Recommended Convective Fraction	Comments		
Occupants, typical office conditions	0.6	0.4	See Table 1 for other conditions.		
Equipment	0.1 to 0.8	0.9 to 0.2	See Tables 6 to 12 for details of equipment heat gain and recommended radiative/convective splits for motors, cooking appliances, laboratory equipment, medical equipment, office equipment, etc. Varies; see Table 3.		
Office, with fan	0.10	0.9			
Without fan	0.3	0.7			
Lighting					
Conduction heat gain					
Through walls and floors	0.46	0.54			
Through roof	0.60	0.40			
Through windows	0.33 (SHGC > 0.5) 0.46 (SHGC < 0.5)	0.67 (SHGC > 0.5) 0.54 (SHGC < 0.5)			
Solar heat gain through fenestration					
Without interior shading	1.0	0.0	Varies; see Tables 13A to 13G in Chapter 15.		
With interior shading					
Infiltration	0.0	1.0			
Athletics	Gymnasium	2000	1800	710	1090

Notes:

1. Tabulated values are based on 75°F room dry-bulb temperature. For 80°F room dry bulb, total heat remains the same, but sensible heat values should be decreased by approximately 20%, and latent heat values increased accordingly.

2. Also see Table 4, Chapter 9, for additional rates of metabolic heat generation.

3. All values are rounded to nearest 5 Btu/h.

^aAdjusted heat gain is based on normal percentage of men, women, and children for the application listed, and assumes that gain from an adult female is

85% of that for an adult male, and gain from a child is 75% of that for an adult male.

^bValues approximated from data in Table 6, Chapter 9, where *V* is air velocity with limits shown in that table.

^cAdjusted heat gain includes 60 Btu/h for food per individual (30 Btu/h sensible and 30 Btu/h latent).

^dFigure one person per alley actually bowling, and all others as sitting (400 Btu/h) or standing or walking slowly (550 Btu/h).

3.7.2 Internal Load: Lighting

In order to determine the hourly cooling load generated by lighting within the room, it has been assumed that a typical fluorescent lighting would be sufficient to keep all area of the room bright. It was also assumed that the fluorescent lighting will be turn on throughout the day as well.

With reference to the owner of a hardware vendor shop, it was known that the total wattage of a widely used fluorescent lighting is 36 W.

With the implementation of radiant time series (RTS) method, the constant hourly heat gain would be categorised into convective portions and also radiant portions by using the coefficients provided in Table 3.7.

Table 3.7: Lighting Heat Gain Parameters for Typical Operating Conditions

(ASHRAE, 2009)

Luminaire Category	Space Fraction	Radiative Fraction	Notes
Recessed fluorescent luminaire without lens	0.64 to 0.74	0.48 to 0.68	<ul style="list-style-type: none"> Use middle values in most situations May use higher space fraction, and lower radiative fraction for luminaire with side-slot returns May use lower values of both fractions for direct/indirect luminaire May use higher values of both fractions for ducted returns
Recessed fluorescent luminaire with lens	0.40 to 0.50	0.61 to 0.73	<ul style="list-style-type: none"> May adjust values in the same way as for recessed fluorescent luminaire without lens
Downlight compact fluorescent luminaire	0.12 to 0.24	0.95 to 1.0	<ul style="list-style-type: none"> Use middle or high values if detailed features are unknown Use low value for space fraction and high value for radiative fraction if there are large holes in luminaire's reflector
Downlight incandescent luminaire	0.70 to 0.80	0.95 to 1.0	<ul style="list-style-type: none"> Use middle values if lamp type is unknown Use low value for space fraction if standard lamp (i.e. A-lamp) is used Use high value for space fraction if reflector lamp (i.e. BR-lamp) is used
Non-in-ceiling fluorescent luminaire	1.0	0.5 to 0.57	<ul style="list-style-type: none"> Use lower value for radiative fraction for surface-mounted luminaire Use higher value for radiative fraction for pendant luminaire

3.7.3 Internal Load: Equipment

For the internal heat load generated by equipment, it has been assumed that the room will be occupy with one laptop for each student. Therefore, the internal heat load generated in the room by the two laptops could be determined by referring to Table 3.8.

By referring to Table 3.8, the internal heat loads generated by the two laptops were 72 W. With the implementation of radiant time series (RTS) method, the constant hourly heat gain would be categorised into convective portions and also radiant portions by using 75 % for convective and 25 % for radiative which are provided in Table 3.8.

Table 3.8: Recommended Heat Gain from Typical Computer Equipment
(ASHRAE, 2009)

Equipment	Description	Nameplate Power Consumption, W	Average Power Consumption, W
Desktop computer ^d	Manufacturer A (model A); 2.8 GHz processor, 1 GB RAM	480	73
	Manufacturer A (model B); 2.6 GHz processor, 2 GB RAM	480	49
	Manufacturer B (model A); 3.0 GHz processor, 2 GB RAM	690	77
	Manufacturer B (model B); 3.0 GHz processor, 2 GB RAM	690	48
	Manufacturer A (model C); 2.3 GHz processor, 3 GB RAM	1200	97
Laptop computer ^b	Manufacturer 1; 2.0 GHz processor, 2 GB RAM, 17 in. screen	130	36
	Manufacturer 1; 1.8 GHz processor, 1 GB RAM, 17 in. screen	90	23
	Manufacturer 1; 2.0 GHz processor, 2 GB RAM, 14 in. screen	90	31
	Manufacturer 2; 2.13 GHz processor, 1 GB RAM, 14 in. screen, tablet PC	90	29
	Manufacturer 2; 366 MHz processor, 130 MB RAM, 14 in. screen)	70	22
	Manufacturer 3; 900 MHz processor, 256 MB RAM (10.5 in. screen)	50	12
Flat-panel monitor ^c	Manufacturer X (model A); 30 in. screen	383	90
	Manufacturer X (model B); 22 in. screen	360	36
	Manufacturer Y (model A); 19 in. screen	288	28
	Manufacturer Y (model B); 17 in. screen	240	27
	Manufacturer Z (model A); 17 in. screen	240	29
	Manufacturer Z (model C); 15 in. screen	240	19

Source: Hosni and Beck (2008).

^aPower consumption for newer desktop computers in operational mode varies from 50 to 100 W, but a conservative value of about 65 W may be used. Power consumption in sleep mode is negligible. Because of cooling fan, approximately 90% of load is by convection and 10% is by radiation. Actual power consumption is about 10 to 15% of nameplate value.

^bPower consumption of laptop computers is relatively small: depending on processor speed and screen size, it varies from about 15 to 40 W. Thus, differentiating between radiative and convective parts of the cooling load is unnecessary and the entire load may be classified as convective. Otherwise, a 75/25% split between convective and radiative components may be used. Actual power consumption for laptops is about 25% of nameplate values.

^cFlat-panel monitors have replaced cathode ray tube (CRT) monitors in many workplaces, providing better resolution and being much lighter. Power consumption depends on size and resolution, and ranges from about 20 W (for 15 in. size) to 90 W (for 30 in.). The most common sizes in workplaces are 19 and 22 in., for which an average 30 W power consumption value may be used. Use 60/40% split between convective and radiative components. In idle mode, monitors have negligible power consumption. Nameplate values should not be used.

3.7.4 External Loads: Heat Transfer Through Opaque Surfaces

The heat transfer through opaque surfaces is a sensible heat transfer process. The heat transfer rate through opaque surfaces in this project are roof and walls and which can be calculated by using Equation (3.1).

$$Q = U \cdot A \cdot \text{Corr.CLTD} \tag{3.1}$$

where

Q = heat load, W

U = overall heat transfer coefficient, W/K

A = heat transfer area of the surface on the side of the conditioned space, m²

Corr.CLTD = corrected cooling load temperature difference, K

For sunlit surfaces, CLTD has to be obtained from the CLTD tables. For surfaces which are not sunlit or which have negligible thermal mass (such as doors), the CLTD value is simply equal to the temperature difference across the wall or roof. Table 3.9 shows the cooling load temperature differences for calculating cooling load from sunlit roof. It was known that the number of roof of the room is one, by studying Table 3.9, the corrected CLTD can be calculated by using Equation (3.2) and Equation (3.3) provided by ASHRAE, 1997.

Table 3.9: Cooling Load Temperature Differences for Calculating Cooling Load from Sunlit Roof (ASHRAE, 1997)

Roof No.	Hour																							
	1	2	3	4	5	6	7	8	9	10	11	12	13	14	15	16	17	18	19	20	21	22	23	24
1	0	-1	-2	-3	-3	-3	0	7	16	25	33	41	46	49	49	46	41	33	24	14	8	5	3	1
2	1	0	-1	-2	-3	-3	-2	2	9	18	27	34	41	46	48	47	44	39	31	22	14	8	5	3
3	7	4	3	1	0	-1	0	3	7	13	19	26	32	37	40	41	41	37	33	27	21	17	13	9
4	9	6	4	2	1	-1	-2	-2	0	4	9	16	23	30	36	41	43	43	41	37	31	25	19	13
5	12	9	7	4	3	2	1	1	3	7	12	17	23	28	33	37	38	38	36	33	28	23	19	15
8	16	13	12	9	8	7	6	6	7	9	12	16	19	23	27	29	31	32	31	29	27	24	21	18
9	18	14	12	9	7	5	3	2	2	4	7	11	15	20	25	29	33	35	36	35	32	29	25	21
10	21	18	15	13	11	8	7	6	5	6	7	9	13	17	21	24	28	31	32	32	31	29	26	23
13	19	17	16	14	12	11	10	9	9	9	11	13	16	18	21	23	26	27	27	27	26	24	22	21
14	19	18	17	15	14	13	12	11	11	11	12	13	16	18	20	22	23	24	25	25	24	23	22	21

Note: 1. Direct application of data

- Dark surface
- Indoor temperature of 25.5°C
- Outdoor maximum temperature of 35°C with mean temperature of 29.5°C and daily range of 11.6°C
- Solar radiation typical of clear day on 21st day of month
- Outside surface film resistance of 0.059 m²·K/W
- With or without suspended ceiling but no ceiling plenum air return systems
- Inside surface resistance of 0.121 m²·K/W

Note: 2. Adjustments to table data

- Design temperatures : $\text{Corr. CLTD} = \text{CLTD} + (25.5 - t_i) + (t_m - 29.4)$

where

t_i = inside temperature and t_m = mean outdoor temperature

t_m = maximum outdoor temperature - (daily range)/2

- No adjustment recommended for color
- No adjustment recommended for ventilation of air space above a ceiling

$$\text{Corr.CLTD} = \text{CLTD} + (25.5 - t_r) + (t_m - 29.4) \quad (3.2)$$

where

Corr.CLTD = corrected cooling load temperature difference, K

CLTD = cooling load temperature difference, K

t_r = inside temperature, m²

t_m = mean outdoor temperature, K

$$t_m = T_{\max} - \frac{\Delta T}{2} \quad (3.3)$$

where

t_m = mean temperature difference, K

T_{\max} = maximum outdoor temperature, K

ΔT = daily temperature range, K

The cooling load temperature difference (CLTD) in Equation (3.2) was calculated by summing up the temperature difference throughout the day and taking the average value. The inside temperature was modified by calculating the average temperature by using the room temperature recorded.

The value of overall heat transfer coefficient for roof can be determined from Table 3.10. The heat transfer through walls can be calculated by using Equation (3.4).

$$Q = U \cdot A \cdot \text{CLTD} \quad (3.4)$$

where

Q = heat load, W

U = overall heat transfer coefficient, W/K

A = heat transfer area of the surface on the side of the conditioned space, m²

CLTD = cooling load temperature difference, K

Table 3.10: Overall Heat Transfer Coefficient of Roof Type (Spitler, Jeffrey and Fisher, 1999)

	Layers (Inside to Outside)	Description	U (Btu/h ft ² °F)	U (W/m ² K)
1	E0 A3 B25 E3 E2 A0	Steel deck with 3.33 in. (85 mm) insulation	0.080	0.454
2	E0 A3 B14 E3 E2 A0	Steel deck with 5 in. (125 mm) insulation	0.055	0.312
3	E0 E5 E4 C12 E3 E2 A0	2 in. (50 mm) h.w. concrete deck with suspended ceiling	0.232	1.317
4	E0 E1 B15 E4 B7 A0	Attic roof with 6 in. (150 mm) insulation	0.043	0.244
5	E0 B14 C12 E3 E2 A0	5 in. (125 mm) insulation with 2 in. (50 mm) h.w. concrete deck	0.055	0.312
6	E0 C5 B17 E3 E2 A0	4 in. (100 mm) h.w. concrete deck with 0.3 in. (8 mm) insulation	0.371	2.107
7	E0 B22 C12 E3 E2 C12 A0	1.67 in. (40 mm) insulation with 2 in. (50 mm) h.w. concrete RTS	0.138	0.784
8	E0 B16 C13 E3 E2 A0	0.15 in. (4 mm) insul. with 6 in. (150 mm) h.w. concrete deck	0.424	2.407
9	E0 E5 E4 B12 C14 E3 E2 A0	3 in. (75 mm) insul. with 4 in. (100 mm) l.w. conc. deck and susp. clg.	0.057	0.324
10	E0 E5 E4 C15 B16 E3 E2 A0	6 in. (150 mm) l.w. conc. dk with 0.15 in. (4 mm) ins. and susp. clg.	0.104	0.591
11	E0 C5 B15 E3 E2 A0	4 in. (100 mm) h.w. concrete deck with 6 in. (150 mm) insulation	0.046	0.261

The cooling load temperature differences for calculating cooling load from sunlit wall and the average cooling load temperature differences (CLTD) for every hour were calculated and the maximum value was used for calculation. Table 3.11 shows the cooling load temperature differences for calculating cooling load from sunlit walls.

Table 3.11: Cooling Load Temperature Differences for Calculating Cooling Load from Sunlit Wall (ASHRAE, 1997)

Wall Face	Hour																							
	1	2	3	4	5	6	7	8	9	10	11	12	13	14	15	16	17	18	19	20	21	22	23	24
N	1	0	-1	-1	-2	-1	4	6	6	7	9	12	14	15	16	16	16	16	15	9	6	4	3	2
NE	1	0	-1	-1	-2	1	13	23	26	24	19	16	15	16	16	16	15	13	11	8	6	4	3	2
E	1	0	-1	-1	-1	1	16	28	34	36	33	27	20	17	17	16	14	11	8	6	4	3	2	
SE	1	0	-1	-1	-2	0	8	18	26	31	32	31	27	22	18	17	16	14	11	8	6	4	3	2
S	1	0	-1	-1	-2	-1	0	2	6	12	18	24	28	29	28	24	19	15	11	8	6	4	3	2
SW	1	0	-1	-1	-1	-1	0	2	4	7	9	14	22	29	36	39	38	34	25	13	7	4	3	2
W	1	1	-1	-1	-1	-1	1	2	4	7	9	12	15	23	33	41	44	44	34	18	9	5	3	2
NW	1	0	-1	-1	-1	-1	0	2	4	7	9	12	14	16	21	28	34	36	31	16	8	5	3	2

Table 3.12 shows the value of overall heat transfer coefficient for sunlit wall.

Table 3.12: Overall Heat Transfer Coefficient of Wall Type (Spitler, Jeffrey and Fisher, 1999)

	Layers (Inside to Outside)	Description	U (Btu/h-ft ² °F)	U (W/m ² K)
1	E0 A3 B1 B13 A3 A0	Steel siding with 4 in. (100 mm) insulation	0.066	0.375
2	E0 E1 B14 A1 A0	Frame wall with 5 in. (125 mm) insulation	0.055	0.312
3	E0 C3 B5 A6 A0	4 in. (100 mm) h.w. concrete block with 1 in. (25 mm) insulation	0.191	1.084
4	E0 E1 B6 C12 A0	2 in. (50 mm) insulation with 2 in. (50 mm) h.w. concrete	0.047	0.267
5	E0 A6 B21 C7 A0	1.36 in. (35 mm) insulation with 8 in. (200 mm) l.w. concrete block	0.129	0.732
6	E0 E1 B2 C5 A1 A0	1 in. (25 mm) insulation with 4 in. (100 mm) h.w. concrete	0.199	1.130
7	E0 A6 C5 B3 A3 A0	4 in. (100 mm) h.w. concrete with 2 in. (50 mm) insulation	0.122	0.693
8	E0 A2 C12 B5 A6 A0	Face brick and 2 in. (50 mm) h.w. concrete with 1 in. (25 mm) insul.	0.195	1.107
9	E0 A6 B15 B10 A0	6 in. (150 mm) insulation with 2 in. (50 mm) wood	0.042	0.238
10	E0 E1 C2 B5 A2 A0	4 in. (100 mm) l.w. conc. block with 1 in. (25 mm) insul. and face brick	0.155	0.880
11	E0 E1 C8 B6 A1 A0	8 in. (200 mm) h.w. concrete block with 2 in. (50 mm) insulation	0.109	0.619
12	E0 E1 B1 C10 A1 A0	8 in. (200 mm) h.w. concrete	0.339	1.925

3.7.5 External Loads: Heat Transfer Through Fenestration

Heat transfer through fenestration is the heat transfer through transparent surface such as window, which includes the heat transfer by conduction due to temperature difference across window and heat transfer due to solar radiation through the window. The heat transfer due to solar radiation through the window can be calculated by formula:

$$Q_{trans} = A_{unshaded} \cdot SHGF_{max} \cdot SC \cdot CLF \quad (3.5)$$

where

Q_{trans} = heat load, W

$A_{unshaded}$ = overall heat transfer coefficient, W/K

$SHGF_{max}$ = solar heat gain factor

SC = shading coefficient

CLF = cooling load factor

In order to consider the conduction heat gains through the door, the glazing solar heat gain coefficients (SHGC) has been assumed zero because the open window area has been completely covered up by the plywood, which appeared opaque.

3.7.6 Infiltration of Outdoor Air and Moisture Transfer

In order to prevent the cooling air from escaping, it was justified that the room would be a closed room with heat gain through infiltration of outdoor air to be negligible. This was due to the fact that the open window area of the room was completely sealed with plywood with no leakage during the installation of geothermal air cooling system.

On top of that, the moisture transfer could be carried out in two paths, which are air leakage due to infiltration or exfiltration and moisture migrates in building envelope. The moisture transfer due to air leakage was justified to be negligible due to the closed room design. The moisture transfer via moisture migrates in building envelope was assumed to be negligible as well as the actual moisture transfer rate is relatively small and often insignificant in the design of typical cooling system.

3.8 Formula for Geothermal Air Cooling System

The formula from Bruce R. Munson, D.F., 2006. *Fundamentals of Fluid Mechanics*. 5th ed. John Wiley & Sons (Asia) Pte Ltd will be used to calculate the heat transfer occurring in the geothermal air cooling system.

3.8.1 Formula for Volume Flow Rate

$$\dot{Q} = \frac{q}{c_p \times \rho \times \Delta T} \quad (3.6)$$

where

\dot{Q} = volume flow rate, m³/s

q = heat gain of the room, kW

c_p = specific heat capacity of air, kJ/kg K

ρ = density of air, kg/m³

ΔT = temperature difference, K

$$Q_a = V \cdot A \quad (3.7)$$

where

Q_a = air flow rate/volume flow rate, m³/s

V = velocity of air, m/s

A = cross sectional area of pipe, m²

$$Q_a = V \cdot \left(\frac{d}{2}\right)^2 \cdot \pi \quad (3.8)$$

where

Q_a = air flow rate/volume flow rate, m³/s

V = velocity of air, m/s

d = inner diameter of pipe, m

$$A_1 Q_1 = A_2 Q_2 \quad (3.9)$$

where

A_1 = cross sectional area of pipe inlet, m²

Q_1 = volume flow rate at pipe inlet, m³/s

A_2 = cross sectional area of exhauster, m²

Q_2 = volume flow rate of exhaust fan, m³/s

3.8.2 Formula for Piping Materials

$$R_{conductive} = \frac{\ln \frac{D_o}{D_i}}{2 \times \pi \times L \times k_p} \quad (3.10)$$

where

$R_{conductive}$ = conductive resistance of pipe per unit length, m K/W

D_o = outer diameter of pipe, m

D_i = inner diameter of pipe, m

L = length of pipe, m

k_p = thermal conductivity of polyvinyl chloride (PVC), W/m K

$$R_{convective} = \frac{1}{\pi \times D_i \times h_{air} \times L} \quad (3.11)$$

where

$R_{convective}$ = convective resistance of pipe per unit length, m K/W

D_i = inner diameter of pipe, m

h_{air} = convective heat transfer coefficient, W/m² K

L = length of pipe, m

$$h_{air} = Nu \times \frac{k_a}{D_i} \quad (3.12)$$

where

h_{air} = convective heat transfer coefficient, W/m² K

Nu = Nusselt number

k_a = thermal conductivity of air, W/m K

D_i = inner diameter of pipe, m

$$Nu = \frac{\left(\frac{f}{8}\right)(Re-1000)Pr}{1+12.7\left(\frac{f}{8}\right)^{0.5}\left(Pr^{\frac{2}{3}}-1\right)} \quad (3.13)$$

where

Nu = Nusselt number

f = friction factor

Re = Reynolds number

Pr = Prandtl number

$$Re = \frac{4\dot{m}}{\pi \times D_i \times \mu} \quad (3.14)$$

where

Re = Reynolds number

\dot{m} = mass flow rate, kg/s

D_i = inner diameter of pipe, m

μ = dynamic viscosity, kg/m s

$$f = \frac{1}{(0.79 \ln Re - 1.64)^2} \quad (3.15)$$

where

f = friction factor

Re = Reynolds number

$$Pr = \frac{c_p \times \mu}{k_a} \quad (3.16)$$

where

Pr = Prandtl number

c_p = specific heat capacity of air, kJ/kg K

μ = dynamic viscosity, kg/m s

k_a = thermal conductivity of air, W/m K

$$q = UA\Delta T = \frac{\Delta T}{R_{Total}} \quad (3.17)$$

where

q = heat gain of the room, kW

U = overall heat transfer coefficient, W/K

A = cross sectional area of pipe, m²

ΔT = temperature difference, K

R_{total} = total resistance of pipe per unit length, m K/W

$$UA = \frac{1}{R_{Total}} = \frac{1}{R_{conductive} + R_{convective}} \quad (3.18)$$

where

U = overall heat transfer coefficient, W/m² K

A = cross sectional area of pipe, m²

R_{total} = total resistance of pipe per unit length, m K/W

$R_{conductive}$ = conductive resistance of pipe per unit length, m K/W

$R_{convective}$ = convective resistance of pipe per unit length, m K/W

$$COP = \frac{Q}{w} \quad (3.19)$$

where

COP = coefficient of performance

Q = heat removed from the room by geothermal air cooling system, W

w = work consumed by the centrifugal fan, W

CHAPTER 4

RESULTS AND DISCUSSION

4.1 Heat Transfer Performance of Different Piping Materials for Experimental Design

The measurement of temperature at both inlet and outlet were being carried out for the four types of pipes. The measurement started from 10.30 am to 5.30 pm, with one hour interval between the measurements. The result was tabulated in Appendices. Table 4.1 shows the average inlet and outlet temperature of for different piping materials.

Table 4.1: Average Inlet and Outlet Temperature of Piping Materials from 26th of March, 2015 to 28th of March, 2015

Date	Type of Pipe							
	Galvanised Iron		PVC		Aluminium		HDPE	
	Inlet	Outlet	Inlet	Outlet	Inlet	Outlet	Inlet	Outlet
26 th of March 2015	35.8	35.2	35.9	34.9	35.6	35.2	35.8	34.7
27 th of March 2015	35.9	35.3	35.5	34.5	35.3	34.9	35.2	34.2
28 th of March 2015	36.0	35.1	36.4	35.3	36.1	35.5	36.7	35.6
Average Inlet Temperature (°C)	35.9	35.2	35.9	34.9	35.7	35.2	35.9	34.8

Sample calculation on PVC pipe:

Average inlet temperature, T_i

$$\begin{aligned}
 &= \frac{T_1 + T_2 + T_3}{3} \\
 &= \frac{35.9 + 35.5 + 36.4}{3} \\
 &= 35.9 \text{ } ^\circ\text{C}
 \end{aligned}$$

Sample calculation on PVC pipe:

Average outlet temperature, T_o

$$\begin{aligned}
 &= \frac{T_1 + T_2 + T_3}{3} \\
 &= \frac{34.9 + 34.5 + 35.3}{3} \\
 &= 34.9 \text{ } ^\circ\text{C}
 \end{aligned}$$

Table 4.2 shows the air velocity for both inlet and outlet of pipe. The average air velocity and average mass flow rate were calculated. Table 4.3 shows the diameter and length of respective pipe.

Table 4.2: Velocity, Average Velocity and Mass Flow Rate of Air

Type of Pipe	Air Velocity (m/s)			Mass Flow Rate (kg/s)
	Inlet	Outlet	Average	
Galvanised Iron	9.2	11.1	10.2	0.002971
PVC	9.0	10.8	9.9	0.002851
Aluminium	8.9	10.9	9.9	0.002408
HDPE	9.0	11.0	10.0	0.002282

Table 4.3: Diameter and Length of Respective Pipe

Type of Pipe	Inner Diameter, D_i	Outer Diameter, D_o	Length of Pipe Covered with Soil
Galvanised Iron	0.0174 m	0.0214 m	1.5 m
PVC	0.0173 m	0.0215 m	1.5 m
Aluminium	0.0159 m	0.0191 m	1.5 m
HDPE	0.0154 m	0.0200 m	1.5 m

Sample calculation on PVC pipe:

Average air velocity, V

$$\begin{aligned}
 &= \frac{V_i + V_o}{2} \\
 &= \frac{9.0 + 10.8}{2} \\
 &= 9.9 \text{ m/s}
 \end{aligned}$$

Mass flow rate of air, \dot{m}

$$\begin{aligned}
 &= \rho AV \\
 &= \rho \times \left[\pi \times \left(\frac{D_i}{2} \right)^2 \right] \times V \\
 &= 1.225 \times \left[\pi \times \left(\frac{0.0173}{2} \right)^2 \right] \times 9.9 \\
 &= 0.002851 \text{ kg/s}
 \end{aligned}$$

Table 4.4 shows the amount of heat being transfer to the soil.

Table 4.4: Amount of Heat Transfer to the Soil

Type of Pipe	$R_{conductive}$ (m K/W)	$R_{convective}$ (m K/W)	I/R_{total} (W/ m K)	Temperature Difference, ΔT (°C)	Heat Transfer, q (W)
Galvanised Iron	4.1191×10^{-4}	0.2913	3.4290	0.7	2.3996
PVC	0.1214	0.2353	2.8035	1	2.8035
Aluminium	8.7640×10^{-5}	0.2512	3.9802	0.5	1.9901
HDPE	0.058	0.2555	3.1898	1.1	3.5088

Sample calculation on PVC pipe:

The following value were assumed.

$$\begin{aligned}
 k_p &= 0.19 \text{ W/m K} \\
 k_a &= 0.0257 \text{ W/m K} \\
 \mu &= 1.5573 \times 10^{-5} \text{ kg/m s} \\
 c_p &= 1.005 \text{ kJ/kg K}
 \end{aligned}$$

Conductive resistance of pipe, $R_{conductive}$

$$\begin{aligned}
 &= \frac{\ln \frac{D_o}{D_i}}{2 \times \pi \times L \times k_p} \\
 &= \frac{\ln \frac{0.02}{0.0175}}{2 \times \pi \times 1.5 \times 0.19} \\
 &= 0.1214 \text{ K/W}
 \end{aligned}$$

Reynolds number, Re

$$\begin{aligned}
 &= \frac{\dot{m}}{\pi \times D_i \times \mu} \\
 &= \frac{4 \times 0.002851}{\pi \times 0.0173 \times 1.5573 \times 10^{-5}} \\
 &= 13473.7644
 \end{aligned}$$

Friction factor, f

$$\begin{aligned}
 &= \frac{1}{(0.79 \ln \text{Re} - 1.64)^2} \\
 &= \frac{1}{(0.79 \ln 13628.1284 - 1.64)^2} \\
 &= 0.029
 \end{aligned}$$

Prandtl number, Pr

$$\begin{aligned}
 &= \frac{c_p \times \mu}{k_a} \\
 &= \frac{1.005 \times 1.5573 \times 10^{-5}}{0.0257} \\
 &= 0.6090
 \end{aligned}$$

Nusselt number, Nu

$$\begin{aligned}
 &= \frac{\left(\frac{f}{8}\right)(\text{Re} - 1000)Pr}{1 + 12.7\left(\frac{f}{8}\right)^{0.5}\left(\text{Pr}^{\frac{2}{3}} - 1\right)} \\
 &= \frac{\left(\frac{0.029}{8}\right)(13473.7644 - 1000)(0.6090)}{1 + 12.7\left(\frac{0.029}{8}\right)^{0.5}\left(0.6090^{\frac{2}{3}} - 1\right)} \\
 &= 35.0914
 \end{aligned}$$

Convective heat transfer coefficient, h_{air}

$$\begin{aligned}
 &= Nu \times \frac{k_a}{D_i} \\
 &= 35.0914 \times \frac{0.0257}{0.0173} \\
 &= 52.13 \text{ W/m}^2 \cdot \text{K}
 \end{aligned}$$

Convective resistance of pipe, $R_{convective}$

$$\begin{aligned}
 &= \frac{1}{\pi \times D_i \times h_{air} \times L} \\
 &= \frac{1}{\pi \times 0.0175 \times 52.0083 \times 1.5} \\
 &= 0.2353 \text{ K/W}
 \end{aligned}$$

Overall heat transfer coefficient, UA

$$\begin{aligned}
 &= \frac{1}{R_{Total}} \\
 &= \frac{1}{R_{conductive} + R_{convective}} \\
 &= \frac{1}{0.1214 + 0.2353} \\
 &= 2.8035 \text{ W/K}
 \end{aligned}$$

Temperature difference, ΔT

$$\begin{aligned}
 &= T_i - T_o \\
 &= 35.9 - 34.9 \\
 &= 1^\circ\text{C}
 \end{aligned}$$

Heat transfer, q

$$\begin{aligned}
 &= UA\Delta T \\
 &= 2.8035 \times 1 \\
 &= 2.8035 \text{ W}
 \end{aligned}$$

From Table 4.4, it can be observed that polyvinyl chloride (PVC) pipe and high-density polyethylene (HDPE) pipe have a favourable heat transfer rate compare to galvanised iron pipe and aluminium pipe. It was noted that the metallic pipe, which are galvanised iron pipe and aluminium pipe have relatively low conductive thermal resistance compared to non-metallic pipe which are polyvinyl chloride (PVC) pipe and high-density polyethylene (HDPE) pipe. This is due to the fact that metallic pipe has thermal conductivity much higher than non-metallic pipe. The thermal conductivity of materials being tested in the experiment was listed in Table 4.5.

Table 4.5: Thermal Conductivity of Materials

Materials	Thermal Conductivity, k (W/m K)
Galvanised Iron	53.3
Polyvinyl Chloride (PVC)	0.19
Aluminium	222
High-density Polyethylene (HDPE)	0.48

By referring to Table 4.5, it was noted that although galvanised iron pipe and aluminium pipe have rather high thermal conductivity, but the performance of heat transfer not necessary be the best. This is due to the fact that the thermal conductivity of these two pipes are much higher than the thermal conductivity of clay soil, which is around 0.45 W/m K at maximum moisture content (Din, 2011). At the beginning of the experiment, the temperature difference at inlet and outlet for galvanised iron pipe and aluminium pipe are rather high, after a short period of time, the temperature difference becomes lower and lower. Galvanised iron pipe and aluminium pipe were under-utilized. In other words, heat accumulation had occurred. The rate of heat rejection from the pipe to the soil is higher than the rate in which the soil is capable of conducting the heat away to the earth reservoir. Consequently, the soil temperature around the pipe increased and heat up the pipe, which in turn, the temperature at the outlet of the pipe would increase. The temperature differences between inlet and outlet of galvanised iron and aluminium pipe were 0.7 °C and 0.5 °C respectively.

High-density polyethylene (HDPE) pipe has a high heat transfer rate among the other materials. This is because high-density polyethylene (HDPE) pipe has a thermal conductivity nearest to the clay soil which is 0.48 W/m K. However, it was found that high-density polyethylene (HDPE) is difficult to form into straight line as compared to polyvinyl chloride (PVC) as shown in Figure 4.1, which caused a lot of trouble during installation of piping system and used up a lot of space in the buried area. Although high-density polyethylene has a slightly higher thermal conductivity than polyvinyl chloride (PVC) pipe and also has a nearest thermal conductivity to the soil, these factors can be compensated by the thickness of polyvinyl chloride (PVC) pipe. The thickness of polyvinyl chloride (PVC) pipe is much smaller as compared to

high-density polyethylene (HDPE) pipe, this may improve and also balance the rate of heat transfer to the soil. In fact, the temperature differences between inlet and outlet of pipe for both polyvinyl chloride (PVC) and high-density polyethylene (HDPE) pipe were $1.1\text{ }^{\circ}\text{C}$ and $1\text{ }^{\circ}\text{C}$ respectively, which was very close to each other. Figure 4.2 summarised the rate of heat transfer of different pipes in the form of graph.



Figure 4.1: High-density Polyethylene Pipe and Polyvinyl Chloride (PVC) pipe

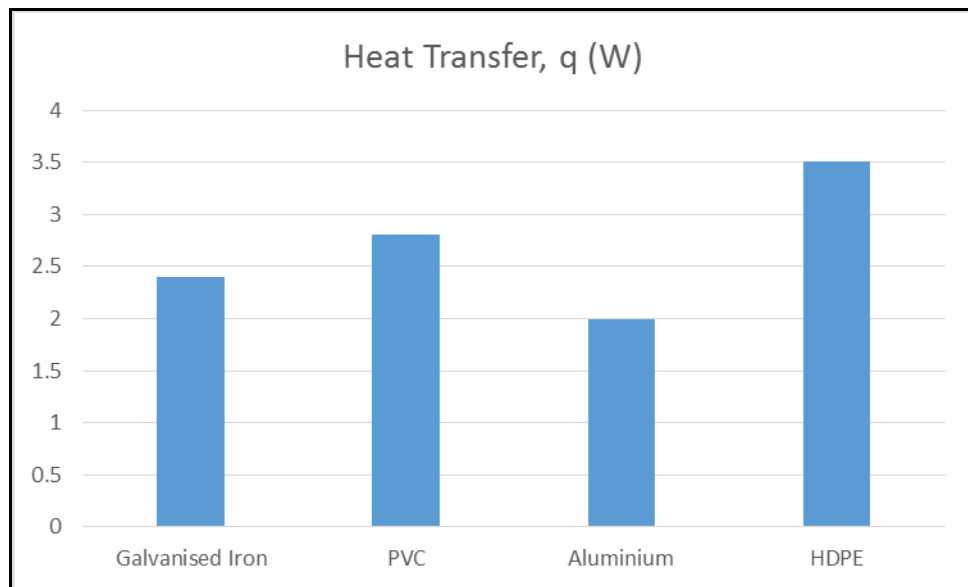


Figure 4.2: Rate of Heat Transfer for Different Pipes

As a conclusion, polyvinyl chloride (PVC) pipe will be chosen to be used in the prototype design of geothermal air cooling system over the other materials as polyvinyl chloride (PVC) pipe is actually sufficient to reject the heat to the ground. From the analysis, the thermal conductivity of material not necessary must be the highest to achieve a favour heat transfer rate, but should be as close as possible to the thermal conductivity of clay soil. Polyvinyl chloride (PVC) pipe also comes with a cheaper price as compared to galvanised iron pipe and aluminium pipe. The price per meter of materials was summarised in Table 3.3.

4.2 Cooling Load Analysis with Implementation of Radiant Time Series (RTS)

4.2.1 Internal Heat Loads by People, Lighting and Equipment

Table 4.6 summarised the total amount of heat gain by people, lighting and equipment.

Table 4.6: Total Amount of Heat Gain by Students, Fluorescent Lighting and Laptops

Type of Internal Heat Load	Total Amount of Heat Gain, W
Students	140
Fluorescent Lighting	36
Laptops	72

It was noted that the total amount of heat gain by the room from the two students, fluorescent lighting and the two laptops can be categorised into two portions, which are radiant portion and convective portion. The radiant portion of heat generated by internal heat loads are the heat generated by the heat source and gradually released to the surroundings as time passes. The convective portion of heat generated by internal heat loads are the heat generated by the heat source and would be directly released to the surrounding as long as the heat is generating. Table 4.7 shows the summary of recommended radiative and convective fraction for respective internal heat loads. The calculated radiant and convective portions of the hourly internal heat loads generated by students, fluorescent lighting and laptops were summarised in Table 4.8.

Table 4.7: Recommended Radiative and Convective Fraction for Students, Fluorescent Lighting and Laptops

Type of Internal Load	Students	Fluorescent Lighting	Laptops
Recommended Radiative Fraction	0.6	0.535	0.25
Recommended Convective Fraction	0.4	0.465	0.75

Table 4.8: Internal Heat Loads Generated in terms of Radiant and Convective Portion

Type of Internal Load		People (W)		Lighting (W)		Equipment (Laptop) (W)	
		Radiative	Convective	Radiative	Convective	Radiative	Convective
Hours	1	84	56	19.26	16.74	18	54
	2	84	56	19.26	16.74	18	54
	3	84	56	19.26	16.74	18	54
	4	84	56	19.26	16.74	18	54
	5	84	56	19.26	16.74	18	54
	6	84	56	19.26	16.74	18	54
	7	84	56	19.26	16.74	18	54
	8	84	56	19.26	16.74	18	54
	9	84	56	19.26	16.74	18	54
	10	84	56	19.26	16.74	18	54
	11	84	56	19.26	16.74	18	54
	12	84	56	19.26	16.74	18	54
	13	84	56	19.26	16.74	18	54
	14	84	56	19.26	16.74	18	54
	15	84	56	19.26	16.74	18	54
	16	84	56	19.26	16.74	18	54
	17	84	56	19.26	16.74	18	54
	18	84	56	19.26	16.74	18	54
	19	84	56	19.26	16.74	18	54
	20	84	56	19.26	16.74	18	54
	21	84	56	19.26	16.74	18	54
	22	84	56	19.26	16.74	18	54
	23	84	56	19.26	16.74	18	54
	24	84	56	19.26	16.74	18	54

4.2.2 External Loads by Heat Transfer Through Opaque Surfaces

The heat transfer rate through roof in this project was calculated using Equation (3.1) and Equation (3.2). The important parameters for Equation (3.2) were calculated.

Cooling load temperature difference, CLTD

$$= \frac{(-1) + (-2) + (-3 \times 3) + 16 + 25 + (33 \times 2) + (41 \times 2) + (46 \times 2) + (49 \times 2) + 24 + 14 + 8 + 5 + 3 + 1}{24}$$

$$= 17.875 \text{ } ^\circ\text{C}$$

Table 4.9 listed the inside room temperature throughout the day from 8 am to 6 pm before the installation of geothermal air cooling system and the average room temperature was calculated.

Table 4.9: Inside Room Temperature from 8 am to 6 pm and Average Room Temperature Before Installation of Geothermal Air Cooling System

Time	Temperature ($^\circ\text{C}$)
0800	28.5
0900	29.8
1000	31.1
1100	32.3
1200	33.8
1300	35.2
1400	36.5
1500	37.3
1600	36.8
1700	35.9
1800	35.0
Average Room Temperature ($^\circ\text{C}$)	33.83

Average inside temperature, t_r

$$= \frac{28.5 + 29.8 + 31.1 + 32.3 + 33.8 + 35.2 + 36.5 + 37.3 + 36.8 + 35.9 + 35.0}{11}$$

$$= 33.83 \text{ } ^\circ\text{C}$$

Table 4.10 shows the surrounding area temperature of the house. The maximum environmental temperature was taken into calculation to calculate the

mean outdoor temperature, which was highlighted. The minimum environmental temperature was highlighted as well for calculating the daily range temperature.

Table 4.10: Surrounding Area Temperature of the House

Time	Temperature (°C)
0800	27.0
0900	27.8
1000	32.0
1100	34.0
1200	35.6
1300	37.0
1400	36.7
1500	36.2
1600	35.5
1700	33.5
1800	30.7

Daily range temperature, ΔT

$$= 37.0 - 27.0$$

$$= 10 \text{ }^\circ\text{C}$$

Mean outdoor temperature, t_m

$$= T_{\max} - \frac{\Delta T}{2}$$

$$= 37.0 - \frac{10.0}{2}$$

$$= 32 \text{ }^\circ\text{C}$$

Corrected cooling load temperature difference, *Corr. CLTD*

$$= CLTD + (25.5 - t_r) + (t_m - 29.4)$$

$$= 17.875 + (25.5 - 33.83) + (32 - 29.4)$$

$$= 12.15 \text{ }^\circ\text{C}$$

Table 4.11 shows the important parameters required to calculate the heat transfer through the roof.

Table 4.11: Parameters of Roof

Parameters	Value
Overall Heat Transfer Coefficient, U	1.317 W/K
Surface Area of Roof, A	11.6081 m ²
Corrected Cooling Load Temperature Difference, $Corr.CLTD$	12.15 K

Surface area of roof, A

$$= 3.22 \times 4.72$$

$$= 15.1984 \text{ m}^2$$

Heat transfer through roof, Q

$$= U \cdot A \cdot Corr.CLTD$$

$$= 1.317 \times 15.1984 \times 12.15$$

$$= 243.1980 \text{ W}$$

The heat transfer through wall was calculated using Equation (3.1). Table 4.12 shows the average cooling load temperature difference throughout the day calculated using Microsoft Excel spreadsheet. The maximum value of average cooling load temperature difference (CLTD) was highlighted. Table 4.13 summarised the important value of parameters for calculating the heat gain through wall.

Table 4.12: Average Cooling Load Temperature Difference for Wall

Wall Face	Hours											
	1	2	3	4	5	6	7	8	9	10	11	12
N	1	0	-1	-1	-2	-1	4	6	6	7	9	12
NE	1	0	-1	-1	-2	1	13	23	26	24	19	16
E	1	0	-1	-1	-1	1	16	28	34	36	33	27
SE	1	0	-1	-1	-2	0	8	18	26	31	32	31
SE	1	0	-1	-1	-2	-1	0	2	6	12	18	24
SW	1	0	-1	-1	-1	-1	0	2	4	7	9	14
W	1	1	-1	-1	-1	-1	1	2	4	7	9	12
NW	1	0	-1	-1	-1	-1	0	2	4	7	9	12
Average CLTD	1	0.125	-1	-1	-1.5	-0.375	5.25	10.375	13.75	16.375	17.25	18.5

Wall Face	Hours											
	13	14	15	16	17	18	19	20	21	22	23	24
N	14	15	16	16	16	16	15	9	6	4	3	2
NE	15	16	16	16	15	13	11	8	6	4	3	2
E	20	17	17	17	16	14	11	8	6	4	3	2
SE	27	22	18	17	16	14	11	8	6	4	3	2
SE	28	29	28	24	19	15	11	8	6	4	3	2
SW	22	29	36	39	38	34	25	13	7	4	3	2
W	15	23	33	41	44	44	34	18	9	5	3	2
NW	14	16	21	28	34	36	31	16	8	5	3	2
Average CLTD	19.375	20.875	23.125	24.75	24.75	23.25	18.625	11	6.75	4.25	3	2

Table 4.13: Parameters of Wall

Parameters	Value
Overall Heat Transfer Coefficient, U	0.88 W/K
Surface Area of Wall 1, A_1	11.6081 m ²
Surface Area of Wall 2, A_2	13.8034 m ²
Cooling Load Temperature Difference, $CLTD$	24.75 K

Surface area of wall 1, A_1

$$= 3.22 \times 3.605$$

$$= 11.6081 \text{ m}^2$$

Heat transfer through wall 1, Q_1

$$\begin{aligned} &= U \cdot A \cdot CLTD \\ &= 0.88 \times 11.6081 \times 24.75 \\ &= 252.8244 \text{ W} \end{aligned}$$

Surface area of wall 2, A_2

$$\begin{aligned} &= (4.72 \times 3.605) - 1.2^2 - (0.85 \times 2.085) \\ &= 13.8034 \text{ m}^2 \end{aligned}$$

Heat transfer through wall 2, Q_2

$$\begin{aligned} &= U \cdot A \cdot CLTD \\ &= 0.88 \times 13.8034 \times 24.75 \\ &= 300.6381 \text{ W} \end{aligned}$$

Total heat transfer through wall

$$\begin{aligned} &= Q_1 + Q_2 \\ &= 252.8244 + 300.6381 \\ &= 553.4625 \text{ W} \end{aligned}$$

4.2.3 Summation of Internal Load and External Load to Obtain Peak Cooling Load

Peak cooling load was obtained by summing up the internal heat load due to the two students, internal load due to fluorescent lighting, and internal load due to the two laptops, external heat transfer through roof and external heat transfer through wall. The calculation was performed as shown.

Peak cooling load, q

$$\begin{aligned} &= (84 + 56) + (19.26 + 16.74) + (18 + 54) + 243.1980 + 533.4625 \\ &= 1024.6605 \text{ W} \end{aligned}$$

Upon the summation of all the calculated internal loads and external loads, the peak cooling load of the room has been obtained. From the calculation shown in

section 4.2.2, the peak cooling load was calculated to be equal to 1024.6605 W. The cooling load for both external loads and internal loads were calculated based on worst condition, which was very hot during the evening. During the hot evening, the sunlight heats up two walls exposed directly to the sunlight. It was known that the heat source was primarily comes from the radiation of heat energy being stored within the walls and roof. By having the peak cooling loads which was the amount of heat that must be removed from the room to maintain the proper temperature in the space, the coefficient of performance of the system can be calculated. Table 4.14 summarised the internal loads and external loads contributed to the total cooling load.

Table 4.14: Internal Loads, External Loads and Total Peak Cooling Load

Internal Loads	Students	140 W
	Fluorescent Lighting	36 W
	Laptops	72 W
External Loads	Heat Transfer through Roof	243.1980 W
	Heat Transfer through Wall	533.4625 W
Total Cooling Loads		1024.6605 W

4.3 Selection of Piping Materials for Prototype System based on Minimum Length and Cost

The minimum length of the geothermal piping system and cost incurred for the geothermal air cooling system which are required to remove the amount of heat of 1024.6605 W was calculated for the four types of materials being studied. It was assumed that the temperature at the outlet of the piping system should be achieved at a value as low as possible, which was equal to 28.2 °C, the average ground temperature at 1.5 m depth. At the same time, the highest temperature at the inlet of the piping system was taken into consideration as well, which was 37.4 °C. The temperatures mentioned were taken from Table 4.17 in Section 4.4.

The minimum length required to dissipate the peak cooling load were calculated. Table 4.15 shows the minimum length required of different materials for achieving the required performance. It was assumed that the inner and outer diameter of pipes are the same as in the experimental design.

Table 4.15: Different Pipes Required Length

Type of Materials	Galvanised Iron	PVC	Aluminium	HDPE
Required Length, <i>m</i>	31.80	52.15	34.02	44.50

Sample calculation on PVC pipe:

Important Parameters:

ρ , kg/m ³	1.225
V_i , m/s	9 – 10
V_o , m/s	16 – 17
D_o , m	0.0215
D_i , m	0.0173
k_p , W/m K	0.19
k_a , W/m K	0.0257
μ , kg/m s	1.5573×10^{-5}
c_p , kJ/kg K	1.005
q , W	1024.6605
ΔT , °C	9.20

Average air velocity, V

$$\begin{aligned}
 &= \frac{V_i + V_o}{2} \\
 &= \frac{9.5 + 16.5}{2} \\
 &= 13 \text{ m/s}
 \end{aligned}$$

Mass flow rate of air, \dot{m}

$$\begin{aligned}
 &= \rho AV \\
 &= \rho \times \left[\pi \times \left(\frac{D_i}{2} \right)^2 \right] \times V \\
 &= 1.225 \times \left[\pi \times \left(\frac{0.0173}{2} \right)^2 \right] \times 13 \\
 &= 0.003743 \text{ kg/s}
 \end{aligned}$$

Conductive resistance of pipe, $R_{conductive}$

$$\begin{aligned}
 &= \frac{\ln \frac{D_o}{D_i}}{2 \times \pi \times L \times k_p} \\
 &= \frac{\ln \frac{0.0215}{0.0173}}{2 \times \pi \times L \times 0.19} \\
 &= \frac{0.1821}{L} \text{ m} \cdot \text{K/W}
 \end{aligned}$$

Reynolds number, Re

$$\begin{aligned}
 &= \frac{4\dot{m}}{\pi \times D_i \times \mu} \\
 &= \frac{4 \times 0.003743}{\pi \times 0.0215 \times 1.5573 \times 10^{-5}} \\
 &= 17691.0358
 \end{aligned}$$

Friction factor, f

$$\begin{aligned}
 &= \frac{1}{(0.79 \ln Re - 1.64)^2} \\
 &= \frac{1}{(0.79 \ln 17691.0358 - 1.64)^2} \\
 &= 0.02699
 \end{aligned}$$

Prandtl number, Pr

$$\begin{aligned}
 &= \frac{c_p \times \mu}{k_a} \\
 &= \frac{1.005 \times 1.5573 \times 10^{-5}}{0.0257} \\
 &= 0.6090
 \end{aligned}$$

Nusselt number, Nu

$$\begin{aligned}
 &= \frac{\left(\frac{f}{8}\right)(Re-1000)Pr}{1+12.7\left(\frac{f}{8}\right)^{0.5}\left(Pr^{\frac{2}{3}}-1\right)} \\
 &= \frac{\left(\frac{0.02699}{8}\right)(17691.0358-1000)(0.6090)}{1+12.7\left(\frac{0.02699}{8}\right)^{0.5}\left(0.6090^{\frac{2}{3}}-1\right)} \\
 &= 43.2836
 \end{aligned}$$

Convective heat transfer coefficient, h_{air}

$$\begin{aligned}
 &= Nu \times \frac{k_a}{D_i} \\
 &= 43.2836 \times \frac{0.0257}{0.0173} \\
 &= 64.2998 \text{ W} / \text{m}^2 \cdot \text{K}
 \end{aligned}$$

Convective resistance of pipe, $R_{convective}$

$$\begin{aligned}
 &= \frac{1}{\pi \times D_i \times h_{air} \times L} \\
 &= \frac{1}{\pi \times 0.0173 \times 64.2998 \times L} \\
 &= \frac{0.28615}{L} \text{ m} \cdot \text{K} / \text{W}
 \end{aligned}$$

Overall heat transfer coefficient, UA

$$\begin{aligned}
 &= \frac{q}{\Delta T} \\
 &= \frac{1024.6605}{9.20} \\
 &= 111.3761 \text{ W / K}
 \end{aligned}$$

Total thermal resistance, R_{total}

$$\begin{aligned}
 &= \frac{1}{UA} \\
 &= \frac{1}{111.3761} \\
 &= 0.008979 \\
 &= R_{conductive} + R_{convective} \\
 &= \frac{0.1821}{L} + \frac{0.2862}{L} \\
 &= \frac{0.4683}{L} \text{ m} \cdot \text{K / W}
 \end{aligned}$$

Required length of pipe, L

$$\begin{aligned}
 &= \frac{0.4683}{0.008979} \\
 &= 52.1476 \text{ m}
 \end{aligned}$$

The minimum length required by the piping system of geothermal air cooling system was calculated. Table 4.16 shows the total price of pipe for respective pipe. From Table 4.16, the length required to dissipate 1024.6605 W of heat by galvanised iron, polyvinyl chloride (PVC), aluminium and high-density polyethylene (HDPE) pipe are 31.80 m, 52.15 m, 34.02 m and 44.50 m respectively, whereby the cost required was calculated to be RM 233.10, RM 139.25, RM 280.00 and RM 48.06 respectively. By comparing the cost required, it was obvious that galvanised iron pipe and aluminium pipe would not be recommended due to the high cost.

For the case of polyvinyl chloride (PVC) and high-density polyethylene (HDPE) pipe, although the minimum length required for both material was calculated, polyvinyl chloride (PVC) pipe needs a longer length and the cost is also

higher. Although the minimum length required by high-density polyethylene (HDPE) pipe is shorter than that of polyvinyl chloride (PVC) pipe, high-density polyethylene (HDPE) pipe may cause a lot of trouble during installation of pipe. It was found that high-density polyethylene (HDPE) pipe is difficult to form into straight line as compared to polyvinyl chloride (PVC) and may use up a lot of space in the buried area. The slightly higher thermal conductivity of high-density polyethylene (HDPE) pipe can be compensated by the thickness of polyvinyl chloride (PVC) pipe. The thickness of polyvinyl chloride (PVC) pipe is much smaller as compared to high-density polyethylene (HDPE) pipe.

Table 4.16: Total Price of Pipe for Respective Pipe

Pipe Material	Price Per Meter (RM)	Required Length, <i>m</i>	Total Price (RM)
Galvanised Iron	7.33	31.80	233.10
PVC	2.67	52.15	139.25
Aluminium	8.23	34.02	280.00
HDPE	1.08	44.50	48.05

4.4 Results of Geothermal Air Cooling System for Prototype Design

In order to analyse the practicability of the designed geothermal air cooling system. The power of exhaust fan was turned on to allow the air to channel into the pipe throughout the day. The temperatures at the inlet of the pipe and outlet of the pipe were recorded throughout the day from 8 am to 6 pm. The average temperature readings was calculated by using the data obtained from 26th of March, 2015 to 28th of March, 2015. Besides that, the ground temperature at 1.5 m beneath the ground was recorded as well. Table 4.17 shows the average temperature at inlet and outlet of the pipe and also the ground temperature at 1.5 m beneath the ground. Figure 4.3 shows the inlet and outlet temperature of the pipe at respective hour.

Table 4.17: Average Temperature of Inlet of Pipe, Outlet of Pipe and 1.5 m Beneath the Ground

Hours	Temperature (°C)			
	Inlet	Outlet	Temperature Difference	1.5 m
0800	28.1	27.4	0.7	27.4
0900	28.7	27.4	1.3	27.3
1000	29.5	27.4	2.1	27.2
1100	31.4	28.0	3.4	27.2
1200	32.7	29.0	3.7	27.8
1300	34.4	29.9	4.5	28.3
1400	35.4	30.5	4.9	28.6
1500	36.9	31.3	5.6	29.0
1600	37.4	31.9	5.5	29.3
1700	35.5	29.8	5.7	29.5
1800	34.3	29.2	5.1	29.0
Average Temperature	33.1	29.3	-	28.2

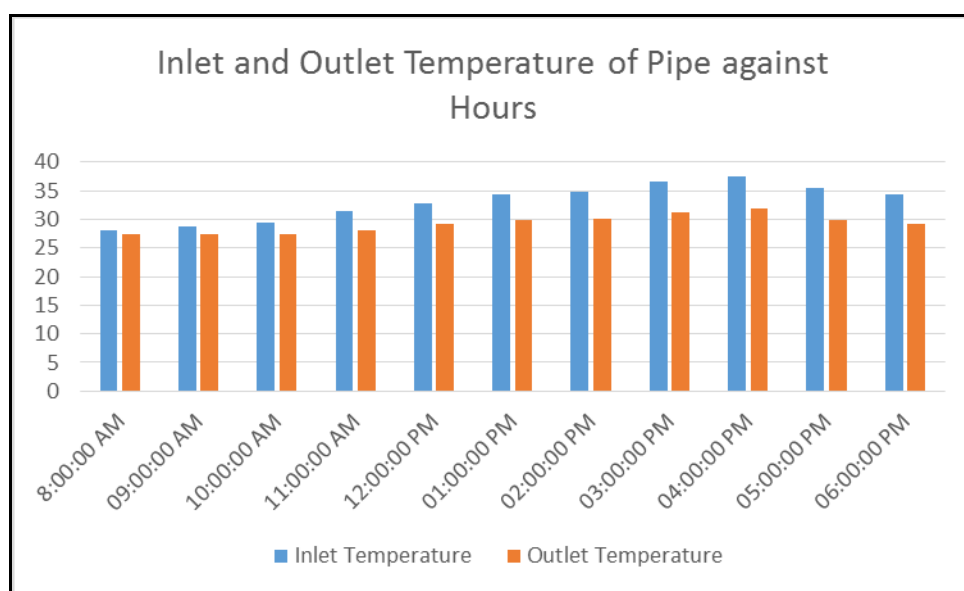


Figure 4.3: Inlet and Outlet Temperature of the Pipe at Respective Hour

From Table 4.17, the average temperature at the inlet of the pipe and outlet of the pipe were calculated to be 33.1 °C and 29.3 °C respectively. The average ground temperature at depth of 1.5 m was calculated to be 28.2 °C. This figure told us that the temperature at the outlet of the pipe would never drop below 28.2 °C, the maximum it can drop was 28.2 °C else the direction of heat transfer would be in an opposite way. Besides that, it was noted that the temperature of the ground at 1.5 m fluctuated between 27 °C to 29 °C. Figure 4.4 shows the ground temperature at 1.5 m beneath the surface of the ground from 8 am to 6 pm. From Figure 4.4, it was found that the temperature at 1.5 m beneath the ground was rather low in the morning, and start to increase from twelve noon until five o'clock in the evening, which shows the highest value of 29.5 °C. This is also the time when the heat source from heat energy stored within the walls and roof are released into the environment of the room. Therefore, the maximum amount of heat that must be removed from the space to maintain the proper temperature in the room is around that time interval.

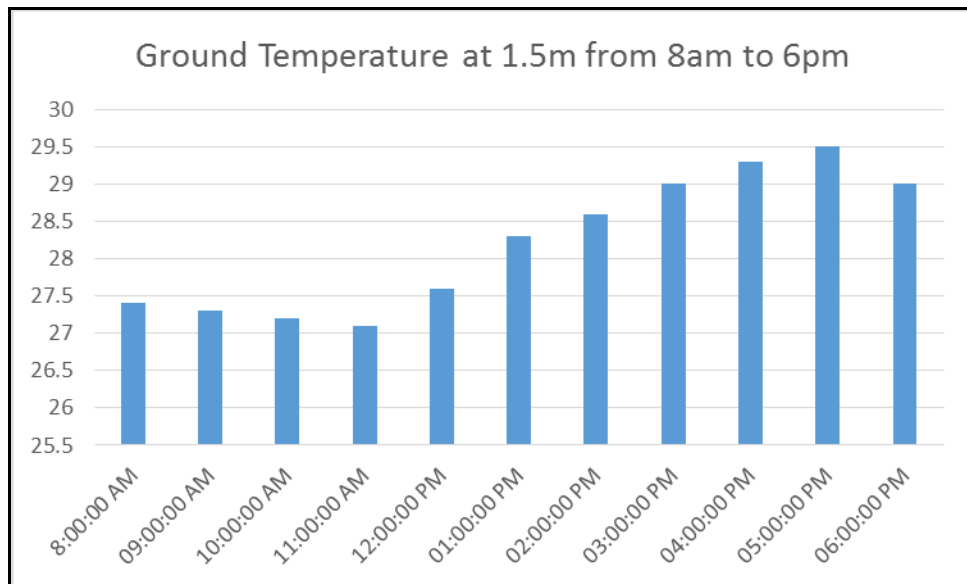
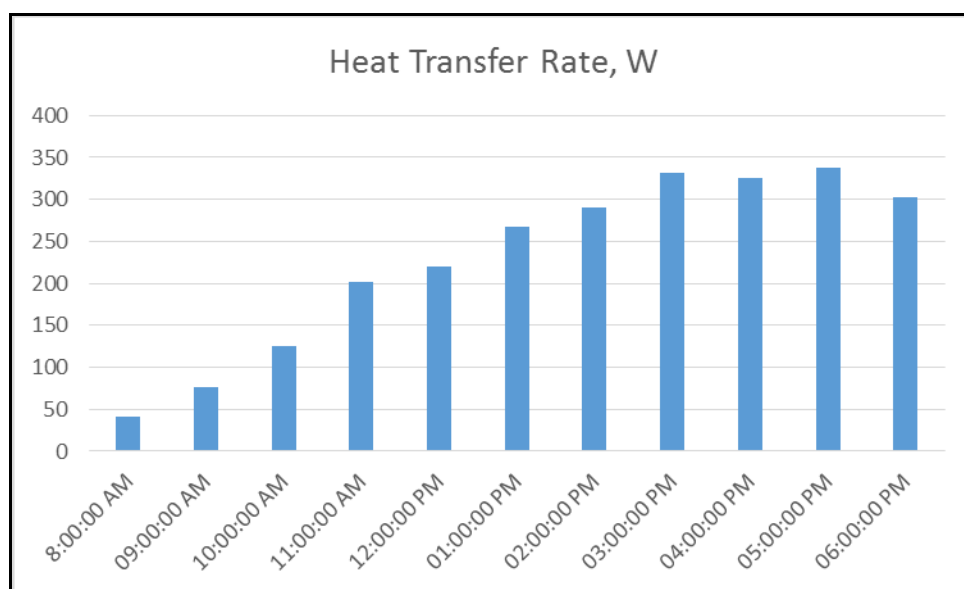


Figure 4.4: Ground Temperature at 1.5 m Beneath Surface of Ground

The air flow through the piping system of geothermal air cooling system was produced with a 50 W DIY centrifugal fan. The centrifugal fan was installed at the outlet of the pipe in the room. The pipe length was measured to be 8.3 m. The heat transfer for every hour from 8 am to 6 pm was calculated and summarise in Table 4.18. Figure 4.5 shows the heat transfer rate with respect to corresponding hours.

Table 4.18: Hourly Temperature Difference and Heat Transfer Rate

Hours	Temperature (°C)			Heat Transfer Rate (W)
	Inlet	Outlet	Temperature Difference	
0800	28.1	27.4	0.7	41.50881
0900	28.7	27.4	1.3	77.08778
1000	29.5	27.4	2.1	124.5264
1100	31.4	28.0	3.4	201.6142
1200	32.7	29.0	3.7	219.4037
1300	34.4	29.9	4.5	266.8423
1400	35.4	30.5	4.9	290.5616
1500	36.9	31.3	5.6	332.0704
1600	37.4	31.9	5.5	326.1406
1700	35.5	29.8	5.7	338.0003
1800	34.3	29.2	5.1	302.4213

**Figure 4.5: Heat Transfer Rate with respect to Corresponding Hours**

By acquiring all the important data collected from the prototype system. The coefficient of performance (COP) of the geothermal air cooling system can be

calculated. Table 4.19 shows the important data required to calculate the coefficient of performance (COP) of the system. The maximum value of heat transfer was taken into consideration to calculate the coefficient of performance (COP) of the geothermal air cooling system.

Table 4.19: Values of Important Parameters

Parameters	Value
ρ , kg/m ³	1.225
V_i , m/s	9 – 10
V_o , m/s	16 – 17
D_o , m	0.0800
D_i , m	0.0756
L , m	8.3
T_o , °C	29.8
T_i , °C	35.5
k_p , W/m · K	0.19
k_a , W/m · K	0.0257
μ , kg/m · s	1.5573×10^{-5}
c_p , kJ/kg · K	1.005
w , W	50

Calculation:

Average air velocity, V

$$\begin{aligned}
 &= \frac{V_i + V_o}{2} \\
 &= \frac{9.5 + 16.5}{2} \\
 &= 13 \text{ m/s}
 \end{aligned}$$

Mass flow rate of air, \dot{m}

$$\begin{aligned}
 &= \rho AV \\
 &= \rho \times \left[\pi \times \left(\frac{D_i}{2} \right)^2 \right] \times V \\
 &= 1.225 \times \left[\pi \times \left(\frac{0.0756}{2} \right)^2 \right] \times 13 \\
 &= 0.0714847 \text{ kg/s}
 \end{aligned}$$

Conductive resistance of pipe, $R_{conductive}$

$$\begin{aligned}
 &= \frac{\ln \frac{D_o}{D_i}}{2 \times \pi \times L \times k_p} \\
 &= \frac{\ln \frac{0.08}{0.0756}}{2 \times \pi \times 8.3 \times 0.19} \\
 &= 0.005709 \text{ K/W}
 \end{aligned}$$

Reynolds number, Re

$$\begin{aligned}
 &= \frac{4\dot{m}}{\pi \times D_i \times \mu} \\
 &= \frac{4 \times 0.0714847}{\pi \times 0.0756 \times 1.5573 \times 10^{-5}} \\
 &= 77308.8037
 \end{aligned}$$

Friction factor, f

$$\begin{aligned}
 &= \frac{1}{(0.79 \ln Re - 1.64)^2} \\
 &= \frac{1}{(0.79 \ln 77308.8037 - 1.64)^2} \\
 &= 0.01902
 \end{aligned}$$

Prandtl number, Pr

$$\begin{aligned}
 &= \frac{c_p \times \mu}{k_a} \\
 &= \frac{1.005 \times 1.5573 \times 10^{-5}}{0.0257} \\
 &= 0.6090
 \end{aligned}$$

Nusselt number, Nu

$$\begin{aligned}
 &= \frac{\left(\frac{f}{8}\right)(Re-1000)Pr}{1+12.7\left(\frac{f}{8}\right)^{0.5}\left(Pr^{\frac{2}{3}}-1\right)} \\
 &= \frac{\left(\frac{0.01902}{8}\right)(77308.8037-1000)(0.6090)}{1+12.7\left(\frac{0.01902}{8}\right)^{0.5}\left(0.6090^{\frac{2}{3}}-1\right)} \\
 &= 133.7773
 \end{aligned}$$

Convective heat transfer coefficient, h_{air}

$$\begin{aligned}
 &= Nu \times \frac{k_a}{D_i} \\
 &= 133.7773 \times \frac{0.0257}{0.0173} \\
 &= 45.4772 \text{ W / m}^2 \cdot \text{K}
 \end{aligned}$$

Convective resistance of pipe, $R_{convective}$

$$\begin{aligned}
 &= \frac{1}{\pi \times D_i \times h_{air} \times L} \\
 &= \frac{1}{\pi \times 0.0756 \times 45.4772 \times 8.3} \\
 &= 0.01115 \text{ K / W}
 \end{aligned}$$

Overall heat transfer coefficient, UA

$$\begin{aligned}
 &= \frac{1}{R_{Total}} \\
 &= \frac{1}{R_{conductive} + R_{convective}} \\
 &= \frac{1}{0.005709 + 0.011115} \\
 &= 59.32 \text{ W / K}
 \end{aligned}$$

Temperature difference, ΔT

$$\begin{aligned}
 &= T_i - T_o \\
 &= 35.5 - 29.8 \\
 &= 5.70 \text{ }^\circ\text{C}
 \end{aligned}$$

Heat transfer, Q

$$\begin{aligned}
 &= UA\Delta T \\
 &= 59.32 \times 5.7 \\
 &= 338.0003 \text{ W}
 \end{aligned}$$

Coefficient of performance, COP

$$\begin{aligned}
 &= \frac{Q}{w} \\
 &= \frac{338.0003}{50} \\
 &= 6.76
 \end{aligned}$$

The geothermal cooling system designed and installed shows a high coefficient of performance (COP) of 6.76. The system was able to bring down the temperature of the room by few degrees. Table 4.20 shows the effect of geothermal air cooling system on the room being cooled. From Table 4.20, it can be observed that the highest temperature drop for the temperature in the tested room is 3.9 °C. Although there was a temperature drop, but it was dropped from 37.3 °C to 33.4 °C, which was not a comfortable temperature for an average person.

Table 4.20: Effect of Geothermal Air Cooling System on Tested Room

Hours	Temperature of the Room (°C)		
	Before Installation	After Installation	Temperature Difference
0800	28.5	28.0	0.5
0900	29.8	29.1	0.7
1000	31.1	29.6	1.5
1100	32.3	30.1	2.2
1200	33.8	31.1	2.7
1300	35.2	32.2	3.0
1400	36.5	32.7	3.8
1500	37.3	33.4	3.9
1600	36.8	33.8	3.0
1700	35.9	33.5	2.4
1800	35.0	33.0	2.0

CHAPTER 5

CONCLUSION AND RECOMMENDATIONS

5.1 Conclusion

The research on geothermal air cooling system installed in University Tunku Abdul Rahman Setapak, Kuala Lumpur being carried out was interested in achieving the stated objectives.

The data in this project was collected through various methods which were experiments and data from works of other researchers. The data analysis was also carried out by using quantitative approach, depending on the research methodology. All the data collected was brought to together to draw conclusions which related back to the objectives the author has set at the beginning of the project report.

In the experimental design stage, polyvinyl chloride (PVC) pipe has been determined to be the suitable piping material for increasing the efficiency of geothermal air cooling system. PVC pipe was chosen over galvanised iron and aluminium pipe because PVC pipe has a better performance in term of heat transfer rate, which was 2.8035 W. Although high-density polyethylene (HDPE) pipe, has a relatively higher heat transfer rate than PVC pipe, however, for the ease of installation and space saving, polyvinyl chloride (PVC) pipe was recommended.

On the other hand, the length required for the four different pipes to remove the peak cooling load of 1024.6605 W was calculated. It was found that the required length for metallic pipe are rather short as compared to non-metallic pipe which are

71.8 m for galvanised iron pipe and 34.02 m for aluminium pipe while for non-metallic pipe are 52.15 m for PVC pipe and 44.50 m for HDPE pipe. By choosing the material based on pricing, galvanised iron pipe pricing at RM 233.10 and aluminium pipe pricing at RM 280.00 will not be under consideration. Although the required length is short for metallic pipe, however, the pricing was too high, which was not economically viable. Residents would consider a commercial air-conditioning system rather than the geothermal air cooling system due to high pricing. PVC pipe was chosen over HDPE pipe for the ease of installation.

During the installation of selected piping material for the geothermal air cooling system, the geothermal air cooling system was able to achieve a COP of 6.76, which was very optimistic. The COP of the geothermal air cooling system was calculated by dividing the heat removal rate of 338.0003 W from the room by power consumption of centrifugal fan, which was 50 W. Although the geothermal air cooling system was able to achieve such high COP, with inlet and outlet temperature of the pipe at 35.5 °C and 29.8 °C respectively, however, the system was not able to cool down the room to a comfortable temperature. During the hot evening, the lowest temperature of the room that the geothermal air cooling system was able to cool down was 33.0 °C.

Therefore, it could be deduced that the geothermal air cooling system in this project has not cool the room to comfortable temperature. However, if efforts were to be carried out in future studies, the heat gain from the room would be able to minimize the temperature inside the room during the hot evening to a comfortable temperature at 24 °C (Ahmad, 2011).

5.2 Recommendations

For the piping material, for a better pipe material to replace PVC pipe, the material should have a thermal conductivity between PVC and HDPE, which was between 0.19 W/m·K and 0.48 W/m·K as we know that the thermal conductivity of soil at maximum moisture capacity was 0.45 W/m·K (Din, 2011). At the same time, the

pipe should also ease the installation of piping material, cheap, and has a low maintenance cost which can last for almost 50 years.

Besides that, the exposition of pipe to external source should also be avoided or eliminated, especially on the section of the pipe where the air coming out from the pipe and channelled back to the room. If the exposition of the pipe to the external heat source cannot be avoided, the installation of a suitable insulation material on the pipe should be carried out and make sure the pipes are as short as possible. In order to shorten the length of the pipe, the geothermal air cooling system should be installed as close as possible to the room where cooling was to be carried out.

In addition, greater installation depth which is expected to provide a lower and much stable ground temperature could be attained to improve the heat rejection to the soil, provided that special drilling technology is available in Malaysia. Detail designs and considerations should be made as well to justify the potential increase in cooling performance over the extra installation cost that would be incurred.

Last but not least, the design calculations could be carried out in a more accurate manner, in the effort to keep on updating the ASHRAE Handbook year by year to have a more accurate database.

REFERENCES

- Ahmad, Z.A., 2011. All govt offices to keep air-cond temperature at 24 °C from now. *The Star Online*, [online] 12 Aug. Available at: <<http://www.thestar.com.my/story/?file=%2F2011%2F8%2F12%2Fnation%2F9285195&sec=nation>> [Accessed 14 January 2015].
- Alam, M.R., Zain, M.F.M. and Kaish, A.B.M.A., 2012. International journal of sustainable construction engineering & technology. *Energy Efficient Green Building Based On Geo Cooling System In Sustainable Construction Of Malaysia*. 3(2), pp. 2180-3242.
- ASHRAE, 2009. *2009 ASHRAE Handbook—Fundamentals*.
- Bruce R. Munson, D.F., 2006. *Fundamentals of Fluid Mechanics*. 5th ed. John Wiley & Sons (Asia) Pte Ltd.
- Din, A.T., & Fazura, Z., 2011. *The study on the soil heat transfer characteristics for the development of a cost-saving underground air cooling system*. Malacca: Faculty of Mechanical Engineering Malaysia.
- Dossat, R.J. and Horan, T.J., 2002. *Principles of refrigeration*. 5th ed. Prentice Hall.
- Gaffar, G.M., 2013. American journal of engineering research. *Experimental Investigation of Geothermal Air Conditioning*. 2(12), pp. 157-170.
- Inalli, M. and Esen, H., 2004. Applied thermal engineering. *Experimental Thermal Performance Evaluation of a Horizontal Ground-Source Heat Pump System*. 24(14-15), pp. 2219-2232.
- Jaswinder, S., 2011. Proceedings first national conference on advances in mech. *Experimental Evaluation of Heat Loss Characteristics of Buried Pipes of Geothermal Air Cooler*, pp. 359-362.
- Lam, H.N. and Wong, H.M., 2005. Proceedings world geothermal congress. *Geothermal Heat Pump System for Air Conditioning in Hong Kong*, (1475), pp. 1-4.

- Pal, R.K., 2013. International journal of engineering sciences & research technology. *Analysis of Geothermal Cooling System for Buildings*. 1(10), pp. 569-572.
- Pal, R.K., 2013. International journal of engineering sciences & research technology. *Analysis of Geothermal Storage of Water*. 2(4), pp. 804-806.
- Pravin, M. and Attar, A.C., 2013. International journal of scientific & engineering research. *Design, Application and Result Analysis of Geothermal Ventilation System*. 4(8), pp. 1990-1999.
- Yuping, H., Yuening, L. and Jian, S., 2009. IEEE thermal investigations of ICS and systems conference (therminic). *Geothermal Cooling Solution Research for Outdoor Cabinet*.
- William D. Callister, Jr., 2007. *Materials Science and Engineering*. 7th ed. New York: John Wiley & Sons, Inc.

APPENDICES

APPENDIX A: Gantt Chart

Gantt Chart of Progress Report

Tasks	Time In Months					
	May 2014	June 2014	July 2014	Aug. 2014	Sept. 2014	Oct. 2014
Registration of FYP title	■	■				
Understand about FYP title		■				
Confirmation of aim and objectives			■			
Journal study and literature review			■	■		
Progress report writing				■		
Preparation for presentation						
Determination on material piping					■	■
Determination on piping configuration						■
Modeling of prototype						■

Tasks	Time In Months						
	Nov. 2014	Dec. 2014	Jan. 2015	Feb. 2015	Mar. 2015	Apr. 2015	May 2015
Determination on piping configuration	■						
Modeling of prototype		■					
Digging of hole							
Installation of piping materials							
Installation of exhaust fan							
Testing of air system			■	■			
Completion of prototype					■		
Troubleshooting of problems encountered						■	
Geothermal System Readings							■
Validation of Geothermal System Readings							■
Final Report Writing/Updating			■	■	■	■	■

APPENDIX B: Tables for On-site Measurement of Temperature for Piping Materials

Table A-1: Temperature Profile of Piping Materials on 26th of March 2015

Material	Temperature (°C)	Morning			Afternoon			Evening		Average Temperature (°C)
		1030	1130	1230	1330	1430	1530	1630	1730	
Galvanised Iron	T_i	32.6	31.7	35.2	38.1	38.0	37.4	37.1	35.9	35.8
	T_o	31.9	30.9	34.7	37.8	37.6	36.9	36.6	35.2	35.2
Polyvinyl Chloride (PVC)	T_i	32.3	33.2	35.5	36.1	37.9	38.4	37.5	35.9	35.9
	T_o	31.7	32.2	34.3	35.5	37.0	37.3	36.3	35.1	34.9
Aluminium	T_i	31.8	32.2	35.2	37.7	36.9	37.6	37.8	35.5	35.6
	T_o	31.3	31.8	34.9	37.3	36.5	37.2	37.3	35.1	35.2
High-density Polyethylene (HDPE)	T_i	31.4	33.5	36.3	36.2	37.6	38.0	37.8	35.7	35.8
	T_o	30.4	32.2	35.2	35.1	36.6	36.9	36.6	34.5	34.7

Table A-2: Temperature Profile of Piping Materials on 27th of March 2015

Material	Temperature (°C)	Morning			Afternoon			Evening		Average Temperature (°C)
		1030	1130	1230	1330	1430	1530	1630	1730	
Galvanised Iron	T_i	33.6	34.5	37.0	37.1	36.7	37.0	37.4	33.9	35.9
	T_o	32.8	34.0	36.4	36.6	36.2	36.5	37.0	33.0	35.3
Polyvinyl Chloride (PVC)	T_i	32.6	34.4	35.5	37.3	36.5	36.0	38.0	33.4	35.5
	T_o	31.8	33.6	34.1	36.4	35.3	35.1	37.0	32.3	34.5
Aluminium	T_i	31.7	33.9	35.5	37.7	36.6	36.0	37.3	33.5	35.3
	T_o	31.4	33.4	35.0	37.2	36.3	35.6	36.9	33.4	34.9
High-density Polyethylene (HDPE)	T_i	31.3	33.3	35.4	37.6	36.7	36.2	37.6	33.8	35.2
	T_o	30.3	32.3	34.3	36.6	35.8	34.9	36.5	33.0	34.2

Table A-3: Temperature Profile of Piping Materials on 28th of March 2015

Material	Temperature (°C)	Morning			Afternoon			Evening		Average Temperature (°C)
		1030	1130	1230	1330	1430	1530	1630	1730	
Galvanised Iron	Inlet Temperature, T_i	32.5	34.5	35.9	38.3	38.4	39.0	37.3	32.1	36.0
	Outlet Temperature, T_o	31.6	33.2	34.0	37.6	38.2	39.0	35.7	31.4	35.1
Polyvinyl Chloride (PVC)	Inlet Temperature, T_i	32.6	34.4	35.5	39.2	39.9	39.0	36.8	33.6	36.4
	Outlet Temperature, T_o	31.8	33.6	34.1	38.2	38.8	37.7	35.4	32.6	35.3
Aluminium	Inlet Temperature, T_i	31.7	33.9	35.5	39.1	39.2	39.7	37.3	32.5	36.1
	Outlet Temperature, T_o	31.0	33.2	34.9	38.6	38.6	39.1	36.6	32.0	35.5
High-density Polyethylene (HDPE)	Inlet Temperature, T_i	31.3	33.3	35.4	40.3	40.6	40.4	39.0	32.9	36.7
	Outlet Temperature, T_o	30.3	32.3	34.3	39.5	39.4	39.4	37.4	32.1	35.6